

Responses to Reviewer Comments: “On the role of soil water retention characteristic on aerobic microbial respiration”

by T.A. Ghezzehei, B. Sulman, C.L. Arnold, N.A. Boggie, A.A. Berhe

November 2, 2018

REVIEWER #1

Major Comments

Comment 1: Page 11, line 4. The authors state that the model of equation 5 can be solved under arbitrary fluctuations of soil water status, i.e. $\theta(t)$ and $\psi(t)$. However, this is not possible to do in close form unless you have a very specific function that shows how θ and ψ change over time; and if you have these functions, it is very unlikely that you will obtain an analytical solution. I would say that this assumption is wrongly stated here, and the authors should acknowledge that the analytical expressions they provide only apply for constant soil water status. Later on page 16, lines 16-17, the authors correctly point out that only numerical solutions are possible for the time-dependent case. This is obviously contradictory to what is stated on page 11.

Response 1: We agree that a complete closed-form solution does not exist for arbitrary fluctuation. We left the integral as is in Eq 11 for this reason. We restated the above sentence as: “The SOM dynamics under arbitrary fluctuation of soil water status (i.e., $\theta(t)$ and $\psi(t)$) can be described by rearranging Eq. (5), subject to initial active pool of SOC $C(t = 0) = C_0$, as...”. Also we added the following sentence right after the equation. “Note that closed form solution for the integral in Eq. 11 exists only at steady water content and water potential status...”

Comment 2: The upper limit of integration in equation 11 is with respect to time, but $K(\theta, \psi)$ is not time-dependent as expressed in equation 12. It seems to me that you may want to integrate over ψ or θ , but not t .

Response 2: The dependence of water content and matric potential was stated in line 4 right above Eq 11, therefore it was implied in equations 11 and 12. We now explicitly show this dependence in Eq 11:

$$C(t) = C_0 \exp \left(-\kappa_o \int_0^t K[\theta(\tau), \psi(\tau)] d\tau \right)$$

Equation 12 is an expression of instantaneous moisture sensitivity, therefore it is not necessary to express the dependence on time.

Comment 3: The solution of equation 5 is $C(t) = C_0 \exp(-kt)$. I assume that your intention is to be able to replace equations 7 to 10 for k as expressed in equation 6. If so, then equation 11 is missing a minus sign and t .

Thank you for pointing out this error. The missing negative sign to Eq 11 was added (see above correction).

Comment 4: Why do you need C_0 in equation 12? I cannot trace it back from the previous equations. Also, what happened to κ ? Shouldnt it go here?

These were typographic errors. The effects of matric potential and accessibility (Eqs. 7 and 10) were inadvertently left out in Eq. 12, but have now been added. These typographic errors in the manuscript were not carried over to the the codes used for calculations. The corrected Eq 12 is:

$$K(\theta, \psi) = e^{\lambda\psi} \left\{ \kappa_{a,\min} + (1 - \kappa_{a,\min}) \left(\frac{\phi - \theta}{\phi} \right)^{1/2} \right\} \left(\frac{\theta}{\phi} \right)^{1/2}$$

Comment 5: Equation 14 doesnt seem right to me. What you probably want is to compute the integral of the respired carbon, i.e. $C_{CO_2} = \int_0^t R(t) d\tau = \int_0^t 1 - C(t) dt$.

We believe the integral in the suggested expression is redundant as $C(t)$ refers to the amount of SOC remaining at any given time (see Eq 11). Therefore, the respired C must be the difference between the initial and remaining C levels; i.e.

$$C_0 - C(t) = C_0 - C_0 \exp \left(\kappa_o \int_0^t K(\tau) d\tau \right) = C_0 \left\{ 1 - \exp \left(\kappa_o \int_0^t K(\tau) d\tau \right) \right\}$$

No change was made in response to this comment.

Comment 6: Another limitation I see in this study is the lack of contrast with a related model that may perform poorly with respect to the newly proposed model. To my knowledge, the only model that can also deal with these multiple limitations is the DAMM model of Davidson et al. (2014). It would be very helpful if the new model is contrasted against DAMM or other model to more explicitly see the advantage of the new method.

Although comparison with another model, such as DAMM, would provide interesting results the comparison would not address the key tenet of this manuscript—to accurately represent the role of soil structure as described by water retention characteristic. A more appropriate test for this model is to compare model performance against experiments in which the soil structure is manipulated such that contrasting water retention characteristics would be achieved for the same soil. Then comparing our model with other models that utilize only water content or matric potential would be meaningful. We hope that publishing this modeling framework would motivate researchers who may have data needed for such comparison to test the our hypothesis. No change was made in response to this comment.

Comment 7: It is my impression that this model requires the availability of water retention curves for its use. This obviously implies an extra effort in terms of data collection. Can the authors elaborate more on this potential limitation of the method?

Yes, this is a limitation. It was made even more clear to us by the availability of only a handful datasets that we could use for testing our model, despite the fact that decomposition experiments at varying moisture statuses have been done numerous times. When WRC data is not available, a practical solution is to use pedo-transfer functions to determine the parameters of WRC. The following statement was added to the last section of the manuscript:

“Application of the proposed model requires availability of water retention characteristic, which may pose practical limitation in cases when water retention data cannot be readily acquired. Availability of only a handful datasets that we could use for testing the proposed model, despite the fact that decomposition experiments at varying moisture statuses have been done

numerous times, is a clear evidence of this challenge. As a stop-gap measure, it is possible to use pedotransfer functions to infer water retention parameters based on routinely measured soil characteristics such as texture, bulk density and organic matter content (Vereecken et al, 1989; Schaap et al, 2011; Van Looy et al, 2017)."

Minor comments

1. Page 6, lines 9-10. Which one is eq. 2 and 3 in fig. 1, i.e. red or blue?

We corrected it as: "In Fig 1, Eq (2) and (3) are illustrated by the solid blue line. We also added the following sentence after Eq 4: In Fig 1, Eq (4) is illustrated by the solid red line. The corresponding bi-modal pore size density function is shown as red-shaded curve."

2. Page 6, line 16. Remove point.

Corrected

3. Equation 7. Here it may be good to remind the reader that matric potential is negative, and therefore k cant be higher than 1.

We dded: "Note that $\kappa_\psi \leq 1$ because matric potential cannot be positive ($\psi \leq 0$)."

4. Page 14, line 8. Can you provide a justification or a reference for this choice of parameter value?

The parameter denotes availability of oxygen under saturated moisture condition and ranges between 0 and 1. A value of 0 means complete lack of O_2 and a value of 1 means maximum O_2 concentration. For lab incubation samples, this value is expected to be dependent on sample size. In field conditions, soil depth is the most important factor that controls a . At this stage the parameter remains the most uncertain part of the proposed model and needs specific experiments to test and parameterize its value. For this paper, we chose the value of $\kappa_{a,\min} = 0.2$ based on the work of Ebrahimi and Or (Global Change Biology, 2016), which corresponds to the dissolved $[O_2]$ at moisture saturation of ≈ 0.9 .

5. Fig 7. What is the difference between the red and the black lines?

The red lines were inadvertently left. They represent a different approach that we tested earlier in the study. They have been removed.

REVIEWER #2

Major Comments

Comment 1: As acknowledged by the authors, the use of combined gas and aqueous diffusion limiting functions to predict respiration-soil water relations had been proposed by Skopp et al. (1990) and used in many occasions later. The matric potential-dependent function capturing reductions in microbial activity is a more novel addition, but similar functions have been recently proposed and used to capture respiration-soil water trends observed in laboratory studies (Yan et al. 2016; Manzoni et al. 2016). It might also be worth looking at other recent papers (some not available at the time this contribution was submitted) using a comparable approach, though with equations derived in different ways (Tang and Riley, 2013; Yan et al. 2018; Moyano et al. 2018). Considering these previous papers, some statements in the Discussion and Conclusions section seem to overstate the novelty of this contribution (P18, L4-5; P19, L9).

Thank you for directing us to the recent sources. We agree with the reviewer about some of the similarities with these sources and made changes accordingly. We added a sentence acknowledging that the diffusion limitation on substrate accessibility that we adopted in Eq. (10) is consistent with prior models (Tang and Riley, 2013; Yan et al. 2016; Manzoni et al. 2016). In the recent paper of Yan et al (2018), the effect of soil texture is captured by the empirical parameters that were fitted to the three soils. It is possible that the effect of SWC is implicitly contained within these tuned parameters as well. Our model was designed to directly address the physical effects of pore size distribution (as described by water retention curve). Other factors that are likely to depend on moisture status including enzyme activity and microbial community structure were not included. This was done to limit the number of tunable parameters and test to what extent water retention characteristic alone can explain moisture sensitivity. The complete moisture sensitivity function is given in Eq. 12 (typographic errors noted by this and the first reviewer have been corrected).

$$K(\theta, \psi) = e^{\lambda\psi} \left\{ \kappa_{a,\min} + (1 - \kappa_{a,\min}) \left(\frac{\phi - \theta}{\phi} \right)^{1/2} \right\} \left(\frac{\theta}{\phi} \right)^{1/2}$$

The differences in moisture sensitivity amongst all the soils con-

sidered in this study are shown in Figure 5. These Figures are comparable in pattern to those of Yan et al (2018; their Figure 5). The major difference being, in our model the shape of these curves is dependent only on the SWC parameters and $\kappa_{a,\min}$. The latter was kept consistent across all soils for simplicity and because the available data was not adequate to test how this parameter varies with depth and/or sample size. In testing our model, the shape of the dimensionless moisture sensitivity curve was prescribed *a priori* based on independently acquired SWC parameters and fixed value of $\kappa_{a,\min} = 0.2$. Thus, the main contribution of our work, which is also a major departure from the models of Yan et al. (2018), Moyano et al. (2018) and their predecessors, is the absence of moisture-sensitivity parameters that are tuned to match with respiration data. This does not negate the importance of moisture dependence of enzymatic and/or microbial activities represented in these other models. To emphasize the above new contribution of this work, we added a new paragraph and a new figure in the discussion section showing the moisture sensitivity curves of the 12 US textural classes. SWC parameters for these soils were derived from Schaap et al (2001).

Comment 2a: The model description is not always clear and there are several inconsistencies in the way parameters are defined. For example, in Eq. 10, the aqueous diffusivity D_W does not have the dimensions of a diffusivity (L^2/T), but is non-dimensional. The symbol C_A in the same equation is not used elsewhere. In Eq. 11-13, which are used to fit the data, C_A does not appear, so accessibility does not play a role, unless C_0 is interpreted as the accessible organic carbon (but that is defined as ‘initial active carbon’). Moreover, the units in Eq. 11-12 do not match up: with K defined as in Eq. 12, the exponent in Eq. 11 is not non-dimensional, but has the same units of C_0 . Towards the end of the manuscript, a “curve lambda” is mentioned (P19, L3), but lambda is only used as a parameter before. Overall, these issues make the reading and interpretation of results difficult.

As stated in the sentence preceding Eq. 10 accessibility “scales with the *relative* aqueous diffusivity”, which implies that it is normalized by diffusivity of saturated soil. The expression in Eq. 10 is that of tortuosity, which by definition is dimensionless. For clarity the sentences above Eq. 10 were revised as follows:

“We assume the fraction of active SOC pool that is accessible to decomposers scales with relative aqueous diffusivity. Therefore, the accessible fraction of the SOC pool is proportional to the liquid phase tortuosity. Here, we use the Bruggeman expression for tortuosity,”

Eq. 12 had typographic errors that caused the confusion raised. The effects of matric potential and accessibility (Eqs. 7 and 10) were inadvertently left out in Eq. 12, but have now been added (see also response to Reviewer #1). In addition, the equation represented a closed-form solution of the right-hand-side of Eq 11 for constant ψ and θ . These was typographic errors in the manuscript but we verified that the codes we used for calculations were correct. The corrected Eq 12 is given above.

Comment 3: Some choices of the soil moisture characteristic curves appear arbitrary. How were unimodal vs. bimodal curves selected? At the dry end of the soil moisture characteristic curves in Fig. 4, for example, there appear to be a sharp decrease in water content possibly a sign that a bimodal curve could work better? I would suggest selecting curves using a more objective criterion based on goodness of fit and robustness (e.g., AIC).

Multimodality of soil water retention curve can arise due to clear distinction between capillary and adsorptive forces. A fairly recent water retention model by Peters (2013) and Iden and Durner (2013) (now known as PetersDurnerIden (PDI) model) suggests that most soils should exhibit bimodality as the drying curve of adsorbed water usually exhibits different pattern from that of water held by capillary forces. The transition from capillary dominated retention to adsorption dominated retention occurs at very low matric potential levels ($< -100\text{ kPa}$). But bimodality can also arise due to structure (e.g., aggregation or biopores) (Durner, 1994) that results in two (or more) distinct populations of pore sizes. The transition between macro-pore dominated retention and micro-pore dominated retention usually occurs at high matric potential. In this paper, the bimodal models were strictly used for soils that exhibit structure related bimodality. An alternative approach would have been to include adsorptive component to all the soils. This would mean that soils that also show additional structural effect need to be fitted with a trimodal model. None of the water retention data that we used have suf-

ficient number of measurements to match the additional degrees of freedom that would be introduced by such model. Therefore we chose to use the classical van Genuchten unimodal model for all soils that exhibit bimodality at the dry end

Minor comments - Please check the whole text for grammar mistakes and inconsistent formatting of citations (e.g., author names in capital, erroneous use of brackets); some of these issues are highlighted below

1. P1, L17: comparing **[Fixed]**
2. P1, L22: Yuste **[Fixed]**
3. P3, L6: nitrification rate. . . correlates **[Fixed]**
4. P6, L1: if alpha refers to matric potential at maximum drainage, I am not sure I understand why D_0 (a function of alpha) refers to the modal rather than maximum pore throat diameter
 - (a) This has been clarified as follows: "...is a parameter that indicates the matric potential at which the water retention curve exhibits the steepest slope". The steepest slope of the curve implies that when a soil is subjected to progressively decreasing matric potential, the largest amount of water will be extracted at $\psi = -\alpha^{-1}$. This also implies that the corresponding pore size D_0 is the most common.
5. P6, L9: "top axis of the figure", which figure? I would refer to the figure number **[Fixed. Also the sentence was moved down so that it comes after Fig 1 was properly introduced]**
6. P6, L15: "unimodal" P6, L16: extra full stop? This sentence appears incomplete **[Fixed. The latter sentence was fixed as: "SWC of soils that exhibit bimodal pore size distribution can be described by sums of two van Genuchten curves (Durner, 1994);"]**
7. P7, L12: check use of brackets - Chowdhury et al. (2011b) **[Fixed]**
8. P7, L16: Watson **[Fixed]**
9. P8, L4: this sentence appears incomplete **[Fixed as "But rather, its effect on SOM decomposition rate (dC/dt) is accounted for through its impact on the accessibility of SOC (Davidson et al., 2012). "]**

10. P11, L17: important to note [Fixed]
11. P14, L8: but in Figure 5, $k_{a,min} = 0.8$ as well P15, L4: what does “explained in its entirety” mean? Based on which performance metric? [The statement in P14, L8 was corrected and now indicated the two values tested in the reported results. The sentence in P15, L4 refers to how the model works. It is not a general statement about moisture sensitivity. In the framework of the proposed model, there are no factors other those explained by the shape of SWC that can explain moisture sensitivity. The sentence was rephrased for clarity as “In the proposed model, sensitivity of SOM decomposition to soil moisture dynamics is explained in its entirety by the SWC, which directly dictates air content, water content and matric potential. ”]
12. P15, L17: “soils that were. . .” [The current phrasing is correct, see emphasized words here: “...individual *samples* of the same soil that *were* incubated at different levels...”. No change was made.]
13. P16: to avoid having incubation duration as a confounding factor, only the first data points from the Arnold et al. (2015) study could be used [That would work if we were only looking for the optimal decomposition rate. But in this model, we also need to know the available SOC pool. Moreover, having multiple measurements over time increases the statistical robustness of the fitted parameter. No change was made.]
14. P16, L21: more than inter-sample differences, the data from Miller et al. (2005) show strong Birch effect (Birch 1958) longer dry periods trigger larger respiration pulses. This effect, which is widespread, cannot be captured by the proposed model. [It is correct that the model does not account for wetting history. In the first wetting cycle, there should not be any difference of wetting-history between the 4-week and 2-week treatments. But, if you look closely at the data it clear that the 2-week rate is consistently lower than the 4-week rate. This can only be attributed to inter-sample differences. We provided two versions of models in which ignored or considered this difference.]

**In both cases the Birch effect was not captured by the model.
We added one statement to highlight this fact.]**

15. P17, L15: delete in the **[Fixed]**
16. P17-18: the structure of the Discussion and Conclusion section is a bit strange, with two introductory paragraphs and a single numbered subsection **[the headed subsection was unnecessary and is now removed.]**
17. P26, last line of the caption: diameter **[Fixed]**
18. Figure 2: check if labels (B) and (C) are correctly placed; the caption is not consistent with the figure and does not explain what panel (d) shows **[Fixed]**
19. P30, caption: no explanation of the difference between top and bottom panel is provided **[Explanation added.]**
20. Figure 6: check panel labels now only (W), (I), and (D) appear as labels **[Explanation added.]**
21. Figure 7: not clear what is the difference between red and black curves **[The red curves were effective saturation curves (on secondary axes) that we plotted for diagnostic purposes and were meant to be commented out in the code. They are now removed.]**
22. Figure A3: bulk density **[Fixed]**
23. Figure A4: what are the numbers in brackets? Is the number of significant digits reasonable? **[These are matric potential values predicted by pedotransfer function. The numbers are now reformatted.]**

References provided by Reviewer #2

1. Birch, H. F. 1958. The effect of soil drying on humus decomposition and nitrogen availability Plant and Soil 10:9-31.
2. Manzoni, S., F. Moyano, T. Katterer, and J. Schimel. 2016. Modeling coupled enzymatic and solute transport controls on decomposition in drying soils. Soil Biology and Biochemistry 95:275-287.

3. Moyano, F. E., Vasi- lyeva, N., and Menichetti, L.: Diffusion based modelling of temperature and moisture interactive effects on carbon fluxes of mineral soils, *Biogeosciences Discuss.*, <https://doi.org/10.5194/bg-2018-95>, in review, 2018.
4. Tang, J. Y., and W. J. Riley. 2013. A total quasi-steady-state formulation of substrate uptake kinetics in complex networks and an example application to microbial litter decomposition. *Biogeosciences* 10:8329-8351.
5. Yan, Z., Liu, C., Todd-Brown, K.E. et al. 2016. Pore-scale investigation on the response of heterotrophic respiration to moisture conditions in heterogeneous soils. *Biogeochemistry* 131: 121134, <https://doi.org/10.1007/s10533-016-0270-0>
6. Yan, Z., B. Bond-Lamberty, K. E. Todd-Brown, V. L. Bailey, S. Li, C. Liu, and C. Liu. 2018. A moisture function of soil heterotrophic respiration that incorporates microscale processes. *Nature communications* 9:2562.

References cited in response to Reviewer #2

1. Durner, W. (1994), Hydraulic conductivity estimation for soils with heterogeneous pore structure, *Water Resour. Res.*, 30, 211223, doi:10.1029/93WR02676.
2. Iden, S. C., and W. Durner (2014), Comment on Simple consistent models for water retention and hydraulic conductivity in the complete moisture range by A. Peters, *Water Resour. Res.*, 50, 75307534.
3. Peters, A. (2013), Simple consistent models for water retention and hydraulic conductivity in the complete moisture range, *Water Resour. Res.*, 49, 67656780.

REVIEWER #3

Major Comments

The manuscript proposes a new modeling framework that integrates the important role of soil water potential on regulating the rate of soil respiration. The model is built on assuming a single pool soil organic matter (SOM) where a first-order kinetics for the rate of SOM decomposition is considered. Authors have expanded the decay rate of SOM (k parameter) to incorporate for the role of biophysical factors, mainly matric potential. This step is performed by a simple and testable exponential relationship between the decay rate and matric potential. The model is then expanded to include variations in oxygen and substrate diffusion as a function of matric potential and soil depth. The simple nature of proposed mathematical framework allows its application for large-scale carbon cycle and climate models while preserving the effects of some of the key biophysical factors. This step is performed nicely in this model by reducing the number of calibration parameters and limiting them to some measurable quantities. The model is ultimately tested again good amount of datasets.

Overall, the technical quality of the manuscript is high and the proposed model has potential to be used in other biogeochemical gas flux models to account for the role of water content and potential, individually. I have some minor comments and recommendations that I believe could help the manuscript to be stronger and accessible for broader audiences.

Comment 1: My main suggestion is to better discuss uncertainties and limitations associated with the previously developed models that the current model aims to address those limitations. At the moment, it is not completely clear how incorporating matric potential into the model improves the model predictions compared to the models without this feature.

Several changes that were in response to the other reviewers' comments will also address this issue. We have clarified what the scope and limitation of the proposed model are (see in particular Comment 7 of Reviewer #1 and Comments 1 and 2 of Reviewer #2). We added a new paragraph and figure added in the end to illustrate how moisture sensitivity curves vary by soil textural class (SWC parameters for the textural class averages were derived from ROSETTA pedotransfer function).

Comment 2: While the idea of using SWC is nice, the implementation and formulation is rather confusing and hard to follow. The main problem might be the inadequate description of the parameters and the links of

parameters through the equations.

There were some typographic errors in the main moisture sensitivity equation (Eq 12) that may have contributed to this lack of clarity. SWC contributes to moisture sensitivity in three ways: effect of water potential, effect of oxygen concentration, and effect of aqueous diffusion. The corrected Eq 12 now clearly shows this combined effect as a product of the three contributions (Eqs 7, 9, and 10, respectively) as explained by Eq. 6.

Comment 3: I also found that the manuscript is a bit bulky in the introduction and method descriptions. I suggest shortening the introduction and methods. While some of the discussions and examples in the introduction and method are informative, I think it might be distracting. For instance examples and discussions on nitrification process could be misleading, since the main story is about respiration and the connection between respiration and nitrification processes is not immediately clear even though both could be aerobic processes. If this part is necessary, I would suggest to provide a discussion on its need.

We agree that the introduction and methods are longer than typical. The current version of the manuscript evolved in response to feedbacks we received after presentations at AGU, EGU and other smaller venues. Because the main thesis of this research falls at the intersection soil biogeochemistry and soil physics, lack of adequate familiarity of concepts on both sides appeared to have been a roadblock in effectively communicating the main message. The discussion around nitrification was needed because Stark and Firestone (1995)—one of the key papers that we relied for developing the water-potential dependence—used activity of nitrifying bacteria as a model system. We added additional statement to clarify this: “They used nitrifying (ammonium oxidizing) bacteria as a model system, in which nitrification rate was considered as a surrogate for microbial activity.”

Comment 4: My other suggestion is to better explain the difference between water content and matric potential, maybe in a schematic. For instance the independent relationship of water potential from water content and its effects on osmotic potential that is discussed in the manuscript is not so clear. This is important motivation of the paper and could be illustrated a little bit more. Meanwhile, the effects of osmotic potential are discussed

in the introduction, but its incorporation in the model is not so clear, even though it has been assumed that Eq. 6 could also account for osmotic potential.

We added clarifying sentences and phrases in the introduction and the methods sections to this effect.

Minor comments:

1. Page 1, Line 21: are strongly correlated heterotrophic respiration rates grammar error? References are not consistent. Some author names are capital and some are not. **[We added the missing preposition ‘with’. The citation database was updated so that all names are capitalized consistently.]**
2. Page 2, line 3: films is dependent grammar? Moisture sensitivity curve is probably not accurate terminology. I suggest to define moisture sensitivity term. **[The incorrect verb was fixed. The term ‘moisture sensitivity’ curve has been used by others as well (e.g., Lawrence, C. R., Neff, J. C. and Schimel, J. P.: Does adding microbial mechanisms of decomposition improve soil organic matter models? A comparison of four models using data from a pulsed rewetting experiment, Soil Biol Biochem Soil Biol Biochem, 41(9), 19231934, 2009).**
3. In page 4 line 18, “biophysical rates”. Here it is not clear what authors mean. **[Corrected as “biophysical factors”].**
4. In Eq. 6 and 7 different k parameters are used. I would suggest to better define these parameters. The current version is a bit confusing. **[More explanations given as suggested].**
5. Section 2.2 “SOM dynamics modeling” is very long that makes it hard to read and follow the method. I suggest breaking down this section into subsections with detailed subheadings. **[Subheadings were added as suggested].**
6. In line 6, page 8, I think the difference between gas and liquid diffusion coefficients of oxygen is about 4 orders of magnitude, I suggest checking the number, once more. **[Corrected as suggested].**
7. Figure A1 is unclear. At the moment, it is unclear what dashed lines mean. PWP and FC could be defined in the caption of the figure.

Bioavailable SOC should be defined. The term has not been defined and discussed in the rest of the manuscript. [We added “The dashed-lines of the Franzluebbers soils denote compressed samples.” Also we defined PWP and FC]

On the role of soil water retention characteristic on aerobic microbial respiration

Teamrat A. Ghezzehei¹, Benjamin Sulman², Chelsea L. Arnold¹, Nathaniel A. Bogie¹, Asmeret Asefaw Berhe¹

5 ¹School of Natural Sciences, University of California, Merced, CA 95340, USA

²Energy and Environmental Sciences Directorate, Oak Ridge National Laboratory, Oak Ridge, TN 37830, USA

10 *Correspondence to:* Teamrat A. Ghezzehei (taghezzehei@ucmerced.edu)

Abstract. Soil water status is one of the most important environmental factors that control microbial activity and rate of soil organic matter (SOM) decomposition. Its effect can be partitioned into effect of water energy status (water potential) on cellular activity, effect of water volume on cellular motility and aqueous diffusion of substrate and nutrients, as well as effect of air content and gas-diffusion pathways on concentration of dissolved oxygen. However, moisture functions widely used in SOM decomposition models are often based on empirical functions rather than robust physical foundations that account for these disparate impacts of soil water. The contributions of soil water content and water potential vary from soil to soil according to the soil water characteristic (SWC), which in turn is strongly dependent on soil texture and structure. The overall goal of this study is to introduce a physically based modelling framework of aerobic microbial respiration that incorporates the role of SWC under arbitrary soil moisture status. The model was tested by comparing it with published datasets of SOM decomposition under laboratory conditions.

1 Introduction

25 Soil moisture is one of the primary physical factors that control microbial activity (Harris, 1981). Short- and long-term temporal variations in soil moisture are strongly correlated with heterotrophic respiration rates (Carbone et al., 2011; Yuste et al., 2007). Therefore, the moisture-decomposition relationship is an

Style Definition: Normal

Deleted:

Deleted: Sulman¹

Deleted: h

Deleted: o

Deleted: (SOM)

Deleted:

Deleted: Soil moisture is one of the primary physical factors that control microbial activity (Harris, 1981). Short- and long-term temporal variations in soil moisture are strongly correlated with heterotrophic respiration rates (Carbone et al., 2011; Yuste et al., 2007). Therefore, the moisture-decomposition relationship is an important determinant of geographic distribution and climatic sensitivity of soil organic carbon (SOC) stocks (Moyano et al., 2013; Schmidt et al., 2011). The microhabitats that influence the community structure and activity of soil microbes (Tecon and Or, 2017) are far too small compared to the macroscopic measures of average soil water status; such as volumetric water content, relative saturation or water holding capacity. At pore and sub-pore scales, the volume and connectivity of water pools and films is dependent on matric potential—a measure of the strength by which water is held in pores and on surfaces. Matric potential determines the thickness of water films (on very dry soils), curvature of the capillary menisci, and the largest drained pore-throat. The relationship between the bulk soil water content and the average matric potential—commonly referred to as soil water characteristic (SWC) or water retention curve (WRC)—is a macroscopic measure of hydrologically relevant pore-size distribution and surface area (Hillel, 1998). As such, it is also a reflection of soil texture, which controls surface area and pore size distribution, and structure, which controls total porosity, and abundance of intra- and inter-aggregate porosity.¹

In process-oriented mathematical models of soil organic matter (SOM) dynamics (Coleman and Jenkinson, 1996; Parton et al., 1998), sensitivity of SOM decomposition to soil moisture is often modelled in terms of functions that scale the maximum decomposition rate as a function of volumetric water content (Sulman et al., 2012). Optimal decomposition rate has been shown to peak at or near *field capacity* (defined interchangeably as matric potential of -30 kPa or water content after a saturated soil is drained for 24–48 hours) with significant reductions in decomposition towards the wet and dry ends of soil moisture range (Franzluebbers, 1999; Linn and Doran, 1984; Monard et al., 2012; Sierra et al., 2017; Tecon and Or, 2017). Typically, such bell-shaped soil moisture sensitivity curves are described using dimensionless polynomial scalars that are calibrated against experimental data (Sulman et al., 2012; Wickland and Neff, 2007).¹

Skopp et al., (Skopp et al., 1990)

important determinant of geographic distribution and climatic sensitivity of soil organic carbon (SOC) stocks (Moyano et al., 2013; Schmidt et al., 2011). The microhabitats that influence the community structure and activity of soil microbes (Tecon and Or, 2017) are far too small compared to the macroscopic measures of average soil water status; such as volumetric water content, relative saturation or water holding capacity. At pore and sub-pore scales, the volume and connectivity of water pools and films are dependent on matric potential—a measure of the strength by which water is held in pores and on surfaces. Matric potential determines the thickness of water films (on very dry soils), curvature of the capillary menisci, and the largest drained pore-throat. The relationship between the bulk soil water content and the average matric potential—commonly referred to as soil water characteristic (SWC) or water retention curve (WRC)—is a macroscopic measure of hydrologically relevant pore-size distribution and surface area (Hillel, 1998). As such, it is also a reflection of soil texture, which controls surface area and pore size distribution, and structure, which controls total porosity, and abundance of intra- and inter-aggregate porosity. In addition, the interaction of microbes with pore water is influenced by the concentration of chemical species that can lower the osmotic potential.

In process-oriented mathematical models of soil organic matter (SOM) dynamics (Coleman and Jenkinson, 1996; Parton et al., 1998), sensitivity of SOM decomposition to soil moisture is often modelled in terms of functions that scale the maximum decomposition rate as a function of volumetric water content (Sulman et al., 2012). Optimal decomposition rate has been shown to peak at or near *field capacity* (defined interchangeably as matric potential of -30 kPa or water content after a saturated soil is drained for 24-48 hours) with significant reductions in decomposition towards the wet and dry ends of soil moisture range (Franzluebbers, 1999; Linn and Doran, 1984; Monard et al., 2012; Sierra et al., 2017; Tecon and Or, 2017). Typically, such bell-shaped soil moisture sensitivity curves are described using dimensionless polynomial scalars that are calibrated against experimental data (Sulman et al., 2012; Wickland and Neff, 2007).

Skopp et al., (1990) proposed one of the earliest conceptual models that attempted to provide mechanistic rationale for why decomposition of SOM exhibits peak rate at certain water content in terms of balance between substrate diffusion and gas diffusion. The model describes aerobic respiratory activity as a process limited by gaseous diffusion and/or aqueous diffusion, at the wet and dry ranges of soil moisture spectrum, respectively,

$$P = \min \left\{ \frac{\gamma D_N(\theta)}{(1 - \gamma) D_O(\theta)} \right\} \quad (1)$$

where P is an index of decay rate, γ is the relative weight (importance) of aqueous diffusion of nutrients, and D_N and D_O are water content (θ) dependent effective diffusion coefficients of nutrients and oxygen, respectively. This model, which results in an inverted 'V'-shaped curve, has sufficient flexibility to capture results from lab incubation experiments. Beyond bulk OM dynamics, this model formulation was shown to capture how nitrification rate of texturally contrasting soils correlates with gas diffusivity under high water content (Schjønning et al., 2003; 2011). Furthermore, the model has been able to capture observed increases in decomposition rate with water content (hence, aqueous diffusion) (Franzluebbers, 1999; Linn and Doran, 1984; Miller et al., 2005; Thomsen et al., 1999).

15 However, the direct influence of water potential (sum of matric and osmotic potentials) on microbial activity and decomposition rate has not been widely adopted in SOM dynamics models (Moyano et al., 2013; 2012). In aqueous media, microorganisms respond to osmotic stress (low osmotic potential) by accumulating electrolytes and small organic solutes that counter the water potential gradient across their membranes (Wood, 2011). The resulting high intracellular osmotic potential inhibits production and
20 activity of enzymes in bacteria (Csonka, 1989; Skujins and McLaren, 1967) as well as fungi (Grajek and Gervais, 1987; Kredics et al., 2000). In unsaturated soils, microorganisms are additionally subjected to matric potential of water, which is comprised of adsorption of thin films on mineral surfaces and capillary attraction of menisci (Hillel, 1998). Thus, enzymatic activity, community composition, and overall activity of bacteria and fungi inhabiting unsaturated soils are significantly impacted by both concentration

Deleted: Beyond bulk OM dynamics, this model formulation was shown to capture how nitrification rate of texturally contrasting soils correlate with gas diffusivity under high water content (Schjønning et al., 2003; 2011). Furthermore, the model has been able to capture observed increases in decomposition rate with water content (hence, aqueous diffusion) (Franzluebbers, 1999; Linn and Doran, 1984; Miller et al., 2005; Thomsen et al., 1999).

Deleted: However, the direct influence of water potential on microbial activity and decomposition rate has not been widely adopted in SOM dynamics models (Moyano et al., 2013; 2012). In aqueous media, microorganisms respond to osmotic stress (low osmotic potential) by accumulating electrolytes and small organic solutes that counter the water potential gradient across their membranes (Wood, 2011). The resulting high intracellular osmotic potential inhibits production and activity of enzymes in bacteria (Csonka, 1989; Skujins and McLaren, 1967) as well as fungi (Grajek and Gervais, 1987; Kredics et al., 2000). In unsaturated soils, microorganisms are additionally subjected to matric potential of water, which is comprised of adsorption of thin films on mineral surfaces and capillary attraction of menisci (Hillel, 1998). Thus, enzymatic activity, community composition, and overall activity of bacteria and fungi inhabiting unsaturated soils are significantly impacted by both concentration of dissolved solutes (osmotic potential) and reduced water content (matric potential) (Chowdhury et al., 2011a; 2011b; Manzoni and Katul, 2014; Stark and Firestone, 1995; Tecon and Or, 2017). It is important to note that soil drying concentrates solutes in pore water, further reducing osmotic potential. However, because water content and matric potential are strongly correlated through the SWC, their effects on microbial respiration and decomposition of SOM are often lumped together or considered interchangeable (Moyano et al., 2012; Sierra et al., 2017).⁴

Unless empirical moisture sensitivity curves

of dissolved solutes (osmotic potential) and reduced water content (matric potential) (Chowdhury et al., 2011a; 2011b; Manzoni and Katul, 2014; Stark and Firestone, 1995; Tecon and Or, 2017). It is important to note that soil drying concentrates solutes in pore water, further reducing osmotic potential. However, because water content and matric potential are strongly correlated through the SWC, their effects on 5 microbial respiration and decomposition of SOM are often lumped together or considered interchangeable (Moyano et al., 2012; Sierra et al., 2017; Moyano et al., 2018; Yan et al., 2018).

Unless empirical moisture sensitivity curves are calibrated individually for each soil, ignoring the independent contributions of water potential and water content on microbial activity is tantamount to discounting the role of soil texture and structure on soil-moisture sensitivity curves. This drawback is 10 especially critical in land surface models that might be applied across many different soil types. In long-term simulations of land-surface processes, the feedback of changes in SOM stocks on soil aggregation and structure—hence, SOM decomposition rate—may not be accurately captured if the effects of water content and water potential are lumped together. It is also an important limitation in modelling SOM dynamics in soils that undergo drastic structural change over short period of time; e.g., via tillage or 15 slaking of dry aggregates during rapid rewetting.

The objective of this study was to provide a modelling framework that allows integration of SWC in SOM dynamics modelling. We introduce a conceptual and mathematical model of SOM dynamics that accounts for the independent roles of soil aeration, water content, and water potential. For simplicity, we limit our analysis and illustration of the model to a single pool of SOM under isothermal conditions.

20 However, the framework can be readily expanded to multiple-pools and dynamic thermal regime.

2 Materials and Methods

Process based SOM dynamics models provide conceptual basis for quantitatively describing the biophysical interactions within the soil system that determine the fate of SOM. However, the model parameters that represent soil and SOM properties and biophysical factors are difficult to determine a 25

Deleted: that

Deleted: rates

priori. Thus, these parameters must be extracted from experimental data via inverse modelling (fitting).

Whether the fitted parameters retain their physical significance when the models are applied to contexts and scales that are not represented in the experimental data is a major challenge for most predictive modelling applications (Finsterle and Persoff, 1997). The pitfalls in this regard include strong correlation

Deleted: (Finsterle and Persoff, 1997).

5 between fitted parameters and over-fitting of experimental data (fitting of random errors at the expense of retaining the ability to generalize). These pitfalls can be partially avoided by reducing the number of tuneable free parameters and/or determining some of the parameters independently of the experimental data that is to be fitted.

The overall goal of the model proposed in this study is to incorporate the role of SWC in modelling of
10 SOM dynamics under arbitrary soil moisture status. To achieve this goal in a robust and generalizable manner, we chose to represent SOM dynamics using a simple single-pool, first-order kinetics. This model relies on only two parameters: the size of the active SOM pool and a constant decay rate. The effect of soil water status and SWC are incorporated in these parameters by relying on well-established relations of multiphase flow and transport concepts and independently fitted SWC curves. This was done without
15 adding new free parameters that are tuned to fit observed SOM decomposition data.

2.1 Soil Water Characteristic

Soil-water characteristic is a constitutive relationship between the soil volumetric water content and matric potential. It embodies the pore-size distribution and as such is a quantitative representation of soil texture and structure. It exerts direct control on macroscopic and microscopic water content distribution,
20 and indirectly influences flow of water, transport of dissolved constituents and gas fluxes. It also has strong bearing on the activity of soil microorganisms and plant roots. SWC is also sensitive to changes in soil structure. The wet end of SWC readily responds to changes in bulk density (e.g. tillage and compaction, root and macro fauna activity, freezing and thawing, drying and rewetting) (Aravena et al., 2013; Ghezzehei, 2000; Or et al., 2000; Ruiz et al., 2015).

Deleted: The wet end of SWC readily responds to changes in bulk density (e.g. tillage and compaction, root and macro fauna activity, freezing and thawing, drying and rewetting) (Aravena et al., 2013; Ghezzehei, 2000; Or et al., 2000; Ruiz et al., 2015).

SWC is typically represented by a monotonic sigmoid function, the most common being van Genuchten's (van Genuchten, 1980) equation

$$\Theta = (1 + (\alpha\psi)^n)^{-m} \quad (2)$$

where $\Theta = (\theta - \theta_r)/(\theta_s - \theta_r)$ is effective water saturation; θ , θ_r , and θ_s are volumetric water content, residual water content, and saturated water content, respectively; ψ [kPa] is matric potential; α^{-1} [kPa] is a parameter that indicates the matric potential at which the water retention curve exhibits the steepest slope; and n ($1 < n < \infty$) and $m = 1 - 1/n$ are shape parameters that reflect the spread of the SWC function. Matric potential can be related to an effective pore-throat diameter using the Young-Laplace law as $D \approx 4\sigma/\psi$, where σ [N m⁻¹] is surface tension of pore water. Therefore, the SWC function (2) can be written in terms of the pore-throat diameter as,

$$F = \left(1 + \left(\frac{D_0}{D}\right)^n\right)^{-m} \quad (3)$$

where $F = \theta/\theta_s$ represents the relative saturation or cumulative pore size distribution. Eq. (3) is a re-interpretation of SWC as cumulative pore size distribution and $D_0 \approx 4\alpha\sigma$ stands for the modal pore-throat diameter. In Fig. 1, Eq. (2) and (3) are illustrated by the solid blue line. The corresponding pore-size density function $f = dF/dD$ is shown as the blue-shaded bell-shaped curve. The pore-throat diameter scale is shown on the top axis of the Fig. 1. This form of SWC is a good approximation for soils with unimodal pore-size distribution.

However, soils with significant level of aggregation, clumping and/or biopores exhibit multimodal pore size distributions—for example with fine intra-aggregate pores and coarse inter-aggregate pores. Such soils can be represented by summation of two or more unimodal pore-size distributions. SWC of soils that exhibit bimodal pore size distribution can be described by sums of two van Genuchten curves (Durner, 1994):

Deleted: SWC is typically represented by monotonic sigmoid function, the most common being van Genuchten's (van Genuchten, 1980) equation

Deleted: α

Deleted: maximum drainage of soil

Deleted: occurs

Deleted:

Deleted: The pore-throat diameter scale is shown on the top axis of the figure.

Deleted: unimodal pore-size distributions. For soils that exhibit bimodal pore size distribution, by sums of two van Genuchten curves (Durner, 1994)

$$\Theta = \sum_{i=1}^2 w_i (1 + (\alpha_i \psi)^{n_i})^{-m_i} \quad (4)$$

where $w_1 + w_2 = 1$ represents the relative weights of the inter- and intra- aggregate pore populations. In Fig 1, Eq (4) is illustrated by the solid red line. The corresponding bi-modal pore size density function is shown as red-shaded curve.

5 It is important to note that water retention is dominated by capillary attraction in the wet end of the SWC curve, approximately $\psi > -10^{-2}$ kPa and $D > 1 \mu\text{m}$, while adsorption of thin water film on mineral surfaces dominates in the dry range (Or and Tuller, 1999). Thus, soil texture is the most important determinant in the dry end of SWC while structure and water-stable aggregation dominate in the wet end. The latter is strongly influenced by amount and nature of SOM, and readily responds to changes in SOM

10 content.

Deleted: (Or and Tuller, 1999).

2.2 SOM Dynamics Modelling

The conceptual basis for our model is that soil organic matter is comprised of a single pool characterized by first-order rate of decomposition

$$\frac{dC}{dt} = -\kappa C \quad (5)$$

15 where C [mg-C/g-SOC₀] is the active C pool remaining at any given time, expressed as a fraction of the total initial SOC and the rate constant κ [day⁻¹] is a measure of SOM decomposition largely driven by living decomposers. Therefore, we consider it to be a composite parameter that accounts for the abundance of decomposer population as well as the activity of an average decomposer. Both of these factors are impacted when soil moisture level changes. Chowdhury et al. (2011b) observed that the

20 abundance of active decomposers declines while maintaining the same level of average activity as water potential dropped from $\psi = 0$ kPa to $\psi = -2000$ kPa. Organisms subjected to low total water potential exhibit reduced population growth as substantial proportion of their energy intake is routed towards

Deleted: (Chowdhury et al., 2011b) observed that the abundance of active decomposers declines while maintaining the same level of average activity as water potential dropped from $\psi = 0$ kPa to $\psi = -2000$ kPa. Organisms subjected to low total water potential exhibit reduced population growth as substantial proportion of their energy intake is routed towards osmo-regulation (Harris, 1981; WATSON, 1970). Upon further drying, however, the population remained constant but the activity declined sharply (Chowdhury et al., 2011a; 2011b). Previously, (Stark and Firestone, 1995) used two independent techniques to evaluate the relative importance of water potential on cytoplasmic dehydration and the role of water content diffusional limitations in controlling rates of nitrification in soil. Nitrification rates in well mixed soil slurries, in which NH₄⁺ was maintained at high concentrations and osmotic potential was controlled by the addition of K₂SO₄, declined exponentially with reduction in water potential (0 to ~ -4000 kPa) of the slurries. In a companion moist soil incubation experiment, in which substrate supply was controlled by the addition of NH₃ gas, they observed that steeper decline in nitrification as a result of combined effects of reduced diffusion and cytoplasmic dehydration. Similarly, (Tresner and Hayes, 1971) showed that in the absence of diffusion limitation the survival probability of fungi declines with water potential. In the proposed model we assume that the diffusion limitation does not directly control the rate constant. But rather, its effect on SOM decomposition rate (dC/dt) through its impact on the accessibility of (Davidson et al., 2012).

Formatted: Font: (Default) Helvetica Neue, Font color: Black, Lowered by 2.5 pt

osmo-regulation (Harris, 1981; Watson, 1970). Upon further drying, however, the population remained constant but the activity declined sharply (Chowdhury et al., 2011a; 2011b). Previously, (Stark and Firestone, 1995) used two independent techniques to evaluate the relative importance of water potential on cytoplasmic dehydration and the role of water content diffusional limitations in controlling soil 5 microbial activity. They used nitrifying (ammonium oxidizing) bacteria as a model system, in which nitrification rate was considered as a surrogate for microbial activity. Nitrification rates in well mixed soil slurries, in which NH_4 was maintained at high concentrations and osmotic potential was controlled by the addition of K_2SO_4 , declined exponentially with reduction in water potential (0 to ~ -4000 kPa) of the slurries. In a companion moist soil incubation experiment, in which substrate supply was controlled by 10 the addition of NH_3 gas, they observed that steeper decline in nitrification as a result of combined effects of reduced diffusion and cytoplasmic dehydration. Similarly, (Tresner and Hayes, 1971) showed that in the absence of diffusion limitation the survival probability of fungi declines with water potential. In the proposed model we assume that the diffusion limitation does not directly control the rate constant. But rather, its effect on SOM decomposition rate (dC/dt) is accounted for through its impact on the 15 accessibility of SOC (Davidson et al., 2012).

Formatted: Font: (Default) Helvetica Neue, Font color: Black, Lowered by 2.5 pt

Another moisture related factor that impacts the rate constant of decomposition by aerobic processes is availability of dissolved O_2 in pore water. Because diffusion of aqueous O_2 is four orders of magnitude slower than that of gaseous O_2 , gas diffusivity is the primary factor that indicates O_2 limitation in SOM dynamics (Skopp et al., 1990). (Schjønning et al., 2003) compared nitrification rate of cores sampled from 20 three soils of contrasting textures and equilibrated at seven matric potential levels, -0.015 to 1.5 kPa, near the wet end of the moisture spectrum. They observed nitrification rates increased in all soils as water content was reduced from saturation, and then decreased with further decline in water content. The initial increase was not correlated with water content or matric potential. However, consistent with the model of (Skopp et al., 1990), relative gas diffusivity was a good predictor of nitrification.

Deleted: decomposition

Deleted: seven

Deleted: (Skopp et al., 1990). (Schjønning et al., 2003)

Deleted: (Skopp et al., 1990).

Based on the above observations, we propose to expand the decomposition rate κ into the product of multiple interacting components that represent biophysical factors,

$$\kappa = \kappa_0 \prod_i \kappa_i \quad (6)$$

where κ_i are dimensionless constants representing the biophysical factors. Here we focus on two such

5 factors, namely matric potential (κ_ψ) and availability of dissolved O_2 (κ_a). The parameter κ_0 [day^{-1}] is an intrinsic (maximum) rate constant and represents the lumped effect of all the remaining unresolved biophysical factors such as temperature, pH, soil mineralogy, OM composition, and nutrient availability. In principle, Eq. (5) can be expanded to accommodate as many variables as needed. This general formulation has been used to represent the effects of various enzyme activities and temperature (Sierra et 10 al., 2017).

2.2.1 Effect of Matric Potential

Here we propose an exponential equation to describe the dependence of soil microbial activity on water potential,

$$\kappa_\psi = e^{\lambda\psi} \quad (7)$$

15 where λ [kPa^{-1}] is a factor that represents the dependence of respiration rate on matric potential. Note that $\kappa_\psi \leq 1$ because matric potential cannot be positive ($\psi \leq 0$). This trend is assumed to account for the decline in population of decomposers as well as reduced per capita activity at very low water potentials. The model fits well the trend of nitrification in slurries observed by (Stark and Firestone, 1995) ($\lambda = 5.8 \times 10^{-4} \text{ kPa}^{-1}$) and the survival probability of fungi in the absence of diffusion limitation observed by 20 (Tresner and Hayes, 1971) ($\lambda = 7.58 \times 10^{-5} \text{ kPa}^{-1}$). Here we utilize the geometric mean of these two coefficients ($\lambda = 2.1 \times 10^{-4} \text{ kPa}^{-1}$) to account for the fact that both bacteria and fungi are involved in soil respiration and that nitrification is more sensitive to resource limitation than respiration (Schjønning et al., 2003; Scott et al., 1996). A comparison between the proposed trend and dimensionless nitrification

Deleted:

Deleted: [0,1]

Deleted: Here we focus only on the limiting effects of water potential and available dissolved oxygen.

Deleted: κ_0

Formatted: Font: (Default) Helvetica Neue, Font color: Black, Lowered by 2.5 pt

Deleted: (Sierra et al., 2017).

Deleted: This trend is assumed to account for the decline in population of decomposers as well as reduced per capita activity at very low water potentials. The model fits well the trend of nitrification in slurries observed by (Stark and Firestone, 1995) ($\lambda = 5.8 \times 10^{-4} \text{ kPa}^{-1}$) and the survival probability of fungi in the absence of diffusion limitation observed by (Tresner and Hayes, 1971) ($\lambda = 7.58 \times 10^{-5} \text{ kPa}^{-1}$). Here we use the geometric mean of these two coefficients ($\lambda = 2.1 \times 10^{-4} \text{ kPa}^{-1}$) to account for the fact that both bacteria and fungi are involved in soil respiration and that nitrification is more sensitive to resource limitation than respiration (Schjønning et al., 2003; Scott et al., 1996). Comparison between the proposed trend and dimensionless nitrification data of (Stark and Firestone, 1995) is shown in Fig 2c. The steepest decline in effective microbial activity occurs in the range $-10^4 \leq \psi \leq -10^2 \text{ kPa}$. Note that although the primary state variable in Eq. (6) is matric potential, it is tacitly assumed that the equation also accounts for decrease in osmotic potential that accompanies concentration of solutes in drying soils (Chowdhury et al., 2011b).

Deleted: use

Deleted: C

data of (Stark and Firestone, 1995) is shown in Fig 2c. The steepest decline in effective microbial activity occurs in the range $-10^4 \leq \psi \leq -10^2$ kPa. Note that although the primary state variable in Eq. (6) is matric potential, it is tacitly assumed that the equation also accounts for the decrease in osmotic potential that accompanies concentration of solutes in drying soils (Chowdhury et al., 2011b).

5 2.2.2 Effect of Dissolved Oxygen

Following (Skopp et al., 1990), we assume the relative dependence of SOM decomposition on dissolved O₂ can be explained by the relative gas-phase diffusivity, which in turn is inversely correlated with tortuosity of the gas phase.

Deleted: Following (Skopp et al., 1990), we assume the relative dependence of SOM decomposition on dissolved O₂ can be explained by the relative gas-phase diffusivity, which in turn is inversely correlated with tortuosity of the gas phase, κ_a :

$$\kappa_a = \frac{D_g}{D_{g,0}} \propto \frac{1}{\tau_a} \quad (8)$$

10 where $D_{g,0}$ and D_g are diffusivities in open air and soil, respectively, and τ_a is tortuosity of the gas phase.

Here we use the well-known, parameter free Bruggeman expression for tortuosity $\tau = a^{-1/2}$, where $a = \phi - \theta$ is air-filled porosity (Pisani, 2011). However, this model does not account for the distance from air-exposed soil surface. In lab incubation studies, short cores and/or cores with large exposed surfaces do not exhibit significant O₂ limitation as the average diffusion distance is short. Conversely, in field 15 conditions, O₂ availability becomes increasingly limiting with depth as transport length increases and cumulative O₂ consumption increases (Angert et al., 2015). Therefore, we add a correction term that accounts for these variations

$$\kappa_a = \kappa_{a,\min} + (1 - \kappa_{a,\min}) \left(\frac{\phi - \theta}{\phi} \right)^{1/2} \quad (9)$$

20 The parameter $\kappa_{a,\min}$ represents the minimum relative SOM decomposition rate when the soil is fully saturated and the O₂ limitation is at its peak. A value of unity implies no O₂ limitation whatsoever and corresponds to very shallow soil. On the other hand, small values of $\kappa_{a,\min}$ are applicable for deeper soils and/or longer cores. Further controlled experiments are needed to ascertain how this parameter varies

Deleted: τ

Deleted: .

Formatted: Font: (Default) Helvetica Neue, Font color: Black, Lowered by 2.5 pt

Deleted: $a^{1/2}$

Deleted: (Pisani, 2011).

Deleted: (Angert et al., 2015).

with depth or sample configuration. The effect of $\kappa_{a, \min}$ on the overall trend of the relative decomposition rate is shown in Fig 2a.

2.2.3 Effect of Water Content on Substrate Accessibility

Another mechanism that water content exerts control over SOM decomposition is through its effect on

5 substrate accessibility to decomposer microorganisms. Aqueous phase diffusivity of soluble substrates becomes increasingly limited as liquid phase connectivity is reduced and transport distance increases (Moldrup et al., 2004; Skopp et al., 1990). We assume the fraction of the active SOC pool that is accessible to decomposers scales with relative aqueous diffusivity. Therefore, the accessible fraction of 10 the SOC pool is proportional to the liquid phase tortuosity. Here, we use the Bruggeman expression for tortuosity,

Deleted:,

Deleted: (Moldrup et al., 2004; Skopp et al., 1990).

Deleted: , which

Deleted: modelled using

Deleted: of the liquid phase

$$\frac{C_A}{C} = \frac{D_w}{D_{w,0}} \propto \frac{1}{\tau_w} = \left(\frac{\theta}{\phi} \right)^{1/2} \quad (10)$$

where C_A stands for the fraction of the active pool of SOC that is accessible to decomposers at the ambient moisture level (Fig 2b). $D_{w,0}$ and D_w are diffusivities in free water and soil, respectively, and τ_w

Deleted:). When the soil pores are saturated with water, the active pool is accessible in its entirety.

15 limitation on substrate accessibility independently from biogeochemical reaction rates (Tang and Riley, 2013; Yan et al. 2016; Manzoni et al. 2016). Eq. 10 implies that the active pool is accessible in its entirety when soil pores are saturated with water. Additionally, it is possible to experience reduction of the absolute quantity of substrate in aqueous phase solution as the increased concentration of dissolved substrates induces sorption (complexation with mineral surfaces) (Šimůnek et al., 2016). This latter effect, 20 which requires inclusion of reactivity of the mineral surfaces, is not incorporated in this study but can be readily added if the requisite properties of the solid phase and SOM are known.

Deleted: (Šimůnek et al., 2016).

2.2.4 Integrated Model

The SOM dynamics under arbitrary fluctuation of soil water status (i.e., $\theta(t)$ and $\psi(t)$) can be described by rearranging Eq. (5), subject to initial active pool of SOC, $C(t = 0) = C_0$, as

Deleted: solving
Deleted:)

$$C(t) = C_0 \exp \left(-\kappa_o \int_0^t K(\theta(\tau), \psi(\tau)) d\tau \right) \quad (11)$$

5 where $K(\theta, \psi)$ is moisture sensitivity function derived by combining modifiers that represent effects of matric potential (Eq. 7), O₂ diffusion (Eq. 9) and accessibility of SOM (Eq. 10),

$$K(\theta, \psi) = e^{\lambda\psi} \left(\kappa_{a,\min} + (1 - \kappa_{a,\min}) \left(\frac{\phi - \theta}{\phi} \right)^{1/2} \right) \left(\frac{\theta}{\phi} \right)^{1/2} \quad (12)$$

Moisture sensitivity calculated using a typical unimodal SWC is illustrated in Fig 2d. Note that a closed form solution for the integral in Eq. 11 exists only at steady water content and water potential status.

Deleted: At

Deleted:, the integral can be evaluated analytically
Formatted: English (UK)

10 leading to a simple closed-form solution,

$$C(t) = C_0 e^{-\kappa_o K(\theta, \psi) t} \quad (13)$$

These solutions have only two free parameters, which are not dependent on water content: initial fraction of the active pool C_0 and the maximum decay rate κ_o . Water content and matric potential are linked via the appropriate SWC equation (Eq. 2 or Eq. 3). Variations in SOM decomposition between different 15 water content levels are explained by independently determined SWC. It is important to note here that characterization of SWC has become more accessible in the past decade with the introduction of apparatus that rely on evaporation rather than regulated pressure (Schindler et al., 2010). Moreover, pedotransfer functions that predict SWC parameters from routinely measured soil properties (e.g., texture, bulk density and SOM) are becoming increasingly more reliable (Zhang and Schaap, 2017)

Deleted: (Schindler et al., 2010).

Deleted: (Zhang and Schaap, 2017)

For comparison with incubation experiments, cumulative CO₂-C evolution can be evaluated by subtracting the dynamic SOC content (Eq. 10 or Eq. 11) from the initial active stock.

$$C_{CO_2}(t) = C_0 - C(t) \quad (14)$$

where C_{CO_2} stands for the cumulative evolved C expressed as fraction of the initial SOC.

5 2.3 Data for Model Testing

Testing the validity of the model in simulating SOM dynamics requires cumulative CO₂-C evolution data from incubation experiments conducted at multiple constant water content levels as well as knowledge of concurrent water content and matric potential values. We obtained laboratory incubation data that meet these requirements, comprising 31 soils, from four published sources. These soils span a wide range of 10 textural classes, SOM concentrations, and soil structural states. Three of the studies were from experiments conducted at steady wetness level and one is from a study involving drying and episodic rewetting. Summary of the datasets used is given in Table 1. The datasets used are described briefly below. The fact that none of the datasets include fully saturated soil is recognized as drawback in the present state model validation.

15 **Arnold et al** (2015): incubated soils from high elevation meadows in the Sierra Nevada, California, at five different water potentials (-10 to -400 kPa) and measured the CO₂ efflux 11 times over 395 days. Soil samples were collected from three distinct hydrologic regions within the meadow area (wet, intermediate and dry) at three depths. SWC data were collected on separate samples using pressure-plate apparatus, which were fitted with bimodal SWC model of (Durner, 1994). The best-fit SWC curves were used to 20 estimate the water content levels of each treatment.

Deleted: SWC data were collected on separate samples using pressure-plate apparatus, which were fitted with bimodal SWC model of (Durner, 1994).

Franzluebbers (Franzluebbers, 1999): collected samples from the surface (0-10 cm) of 15 variably eroded soils of the Madison-Cecil-Pacolet, near Farmington GA. Samples were packed into bottles at two bulk density levels: naturally-settled and lightly-compressed. The resulting 30 distinct soils were

Deleted: Franzluebbers (Franzluebbers, 1999):

incubated at eight water content levels and CO₂ efflux was measured three times over incubation period of 24 days. Matric potential of the samples were measured at the end of the incubation experiment by the filter-paper method. A digitized version of this dataset was published as supplemental material by (Moyano et al., 2012).

Deleted: (Moyano et al., 2012).

5 **Don** (Moyano et al., 2012): additionally, a previously unpublished dataset set by A. Don, that included a 30-day incubation of one soil at five water content levels was obtained from supplemental dataset published by (Moyano et al., 2012). CO₂ efflux data was provided hourly. Matric potential values were inferred from a unimodal SWC curve (van Genuchten, 1980) that was estimated using the pedotransfer function ROSETTA (Schaap et al., 2001).

10 **Miller et al** (Miller et al., 2005): performed a laboratory incubation to evaluate the impact of short-term fluctuations in soil moisture on long-term carbon and nitrogen dynamics. The study was designed to mimic seasonal wetting of dry soils that is characteristic to many arid and semi-arid environments. Sandy clay loam soil samples collected from Sequoia National Park, with C concentration of 2.3%, were incubated in centrifuge tubes. The tubes were wetted to 60% water holding capacity (WHC) and then 15 allowed to dry by evaporation until they were due for rewetting treatment. WHC was defined as the gravimetric water content of saturated soil allowed to drain for 6 hours. Four and two week of rewetting intervals were tested over a 16 week incubation period. Daily CO₂ efflux and water content (expressed in terms of WHC) were provided. The corresponding matric potential values were inferred from a unimodal SWC curve (van Genuchten, 1980) representative for the textural class (Schaap et al., 2001).

Deleted: Don (Moyano et al., 2012): additionally, a previously unpublished dataset set by A. Don, that included a 30-day incubation of one soil at five water content levels was obtained from supplemental dataset published by (Moyano et al., 2012). CO₂ efflux data was provided hourly. Matric potential values were inferred from a unimodal SWC curve (van Genuchten, 1980) that was estimated using the pedotransfer function ROSETTA (Schaap et al., 2001).¹ Miller et al (Miller et al., 2005):

20 2.4 Fitting of Model to Data

The first step of fitting the model to experimental data involves calculating the concurrent water content and matric potential levels at all times as described above. For each of the unique soil types considered, the cumulative CO₂ efflux data from all the different water content levels were fitted together by optimizing initial fraction of the active pool C_0 and the maximum decay rate κ_* , using non-linear

Deleted: (van Genuchten, 1980) representative for the textural class (Schaap et al., 2001).

Levenberg–Marquardt algorithm implemented in the **minpack** package (Elzhov et al., 2016) of R (R Core Team, 2017). For all the soils used in this study, we tested two values of the parameter that represents O₂ limitation in saturated soils ($\kappa_{a,\min} = 0.2$ and $\kappa_{a,\min} = 0.8$). The data-model comparisons reported are $\kappa_{a,\min} = 0.2$, which corresponds to 90% O₂ in the single aggregate level model of Ebrahimi and Or (2016). The relationship between $\kappa_{a,\min}$ and soil depth, soil type, and sample size (for lab experiments) needs further investigation.

Deleted: (Elzhov et al., 2016) of R (R Core Team, 2017). For all the soils used in this study, the parameter that represents O₂ limitation in saturated soils was set to $\kappa_{a,\min} = 0.2$. Validity of this estimate and its sensitivity to soil depth and soil type

Formatted: Font: (Default) Helvetica Neue, Font color: Black, Lowered by 3 pt

3 Results

Simultaneously measured water content and matric potential data from the studies of Arnold et al. and Franzluebbers (Arnold et al., 2015; Franzluebbers, 1999) along with the best-fit bimodal and unimodal

10 SWC curves are reported in Figs. 3 and 4, respectively. The best SWC parameters of all the soils used in this study are reported in Table A1. The SOM-rich meadow soils of Arnold et al. (2015) were developed in cold, high-altitude environment where estimated annual input of SOM far exceeds decomposition. In these soils, SOM content and porosity decrease with depth in all three hydrologic regimes. SOM and porosity across the three sites are ranked as wet >intermediate>dry. All the meadow soils studied exhibit 15 two distinct pore size classes representing (a) large pores between decomposing fibers of organic matter (in the surface peats) and between aggregates (in the subsoils) and (b) finer pores between processed SOM and mineral fractions. The macropores of these soils drain when subjected to low suction (approx. -5 kPa). However, the soils remain fairly wet until they are subjected to matric potentials lower than approx. -300 kPa.

20 The mineral soils in contrast, exhibited unimodal SWC (Franzluebbers, 1999). The compressed samples had slightly lower porosity than their naturally settled counterparts, across all textures investigated. The water content decreased continuously as the matric potential was lowered progressively. However, the compressed soils needed lower matric potential to drain to the same level of wetness. This indicates that compression caused the pores to shrink across most of the pore-size distribution.

Deleted: and Franzluebbers (Arnold et al., 2015; Franzluebbers, 1999) along with the best-fit bimodal and unimodal SWC curves are reported in Figs.

Deleted: The mineral soils in contrast, exhibited unimodal SWC (Franzluebbers, 1999).

In the proposed model, sensitivity of SOM decomposition to soil moisture dynamics is explained in its entirety by the SWC, which directly dictates air content, water content and matric potential. Moisture sensitivity curves of all soils calculated using as Eq. (11) are depicted in Fig. 5. The difference between the soils with unimodal and bimodal SWC curves is mostly reflected in the water potential range for peak decomposition. In addition, compaction results in shift of the moisture sensitivity curves to the dry end, which is a reflection of reduced of mean pore size.

Temporal CO₂ evolution data for a subset of meadow soils (0-10 cm) are compared with best-fit model simulations in Fig 6. We assumed compaction does not alter the optimal decay rate and active pool. Thus, the datasets from the naturally settled and compacted samples were fitted with common parameters. As indicated above, only the initial fraction of the active pool C_0 and the optimal decomposition rate κ_* were optimized for each of the soils. The complete set of best-fit plots and fitted parameters are given Fig A2.

For the mineral soils of Franzluebbers (Franzluebbers, 1999), the final SOC loss during 24-day incubation are compared with model fits in Fig 7. The corresponding temporal CO₂ evolution data and best-fit model simulations for all the mineral soils are depicted in Fig A3. Bulk density levels of individual samples of the same soil that were incubated at different levels of matric potential were not consistent. Bulk densities of individual samples are indicated within each plot subpanel in Fig A3. Due to the variation in bulk densities, the differences between compacted and naturally settled samples were not consistent across the matric potential spectrum. Therefore, in fitting SWC curves to the soil water content and matric potential, inter-sample heterogeneities were not accounted for. The mismatch between measured and simulated CO₂ evolution includes this discrepancy. Temporal CO₂ evolution data and best-fit model simulations for all the mineral soil of Don (Moyano et al., 2012) are depicted in Fig A4. The best-fit model parameters for all the soils are provided in Table A1.

The best-fit optimal decay rates for all the steady moisture experiments are plotted against SOC, active SOC pool C_0 , and incubation period in Fig 8. Recall that the duration of the incubation experiments of

Deleted: The model
Deleted: in this study suggests that
Deleted: represents concurrent states of

Deleted: For the mineral soils of Franzluebbers (Franzluebbers, 1999),...

Deleted: y
Deleted: As a result
Deleted: However
Deleted: the
Deleted: were fitted
Deleted: by ignoring these
Deleted: (Moyano et al., 2012)

Franzluebbers (Franzluebbers, 1999) and Don (Moyano et al., 2012) were much shorter than that of

Deleted: (Franzluebbers, 1999) and Don (Moyano et al., 2012) were much shorter than that of Arnold et al.

Arnold et al. (2015) (24 and 31 days vs 395 days, respectively). Comparing Fig 8b and 8c suggests that the fraction of the SOC stock involved in decomposition (size of the active pool) increases with incubation period. This is to be expected as longer incubation period allows pools with slower decay rates to contribute at an observable rate. Therefore, the average decay rate decreases with incubation period (Fig 8c), as the model used in this study considers only one pool. The apparent correlation between the fitted parameters (Fig 8b) is partially explained by this phenomenon as well.

Finally, comparison of the measured CO_2 evolution data from all the three studies (1375 data points representing 40 different soils) are compared with the model fits in logarithmic scale and linear-scale (inset) in Fig 9. The colour intensity of the points reflects density of data points. Over all, the model is in excellent agreement with experimental observations across the full range of measured data.

Comparisons of CO_2 evolution data of Miller et al. (Miller et al., 2005) under drying and rapid-wetting condition with model simulations are shown in Fig 10. The fluctuation in the CO_2 evolution rate is explained by the dynamics of water content (Fig 10a) and matric potential. Because a closed-form solution does not exist for arbitrary fluctuations of soil moisture, the integral in Eq. (10) was evaluated numerically. Two sets of model fits were performed. In the first, data from the two- and four-week rewetting intervals were fitted together using one set of initial fraction of the active pool C_0 and the optimal decomposition rate κ_0 (Fig 10b). However, as shown in Fig 10, the two intervals started with a distinct difference at the initial measurement period, which is assumed to reflect significant inter-sample difference. Therefore, a second model fit was conducted, by treating the two intervals separately (Fig 10c). The efflux of CO_2 immediately after re-wetting was consistently much higher than subsequent readings at comparable wetness level. This effect of drying and re-wetting, the Birch (1958) effect, is not accounted for in the proposed model.

Deleted: between

Deleted: (Miller et al., 2005)

Deleted:

4. Discussion

In the remainder of the discussions, soil matric potential is considered as the primary independent state variable, while water content and decomposition modifiers are all functions that depend on water potential. For all the soils investigated, the peak decomposition rate was approximately 60% (Fig 5) of the optimal rate that would occur if aqueous diffusion, gaseous diffusion and water potential were not limiting. However, in soils where one or more of these factors are limiting across the spectrum of possible moisture range, SOM decomposition occurs under a suboptimal rate. The individual contributions of these limiting factors are shown in Fig A1. The effect of water potential is assumed to be due to matric potential only. This assumption ignores increase in solute concentration during drying and associated decrease in matric potential. The limiting effects of aqueous and gaseous diffusion directly depend on water content and porosity, therefore depending on SWC.

Soils with a broad range of pore size distribution drain incrementally over a wide range of matric potential, thus maintaining a broad range of favourable moisture status. This is clearly demonstrated in the contrast between the moisture sensitivity of the meadow soils and the rest of the soils. Most of the meadow soils show peak decomposition between -1000 kPa and -10 kPa, with rapid drop in decomposition under saturated conditions. Recall that the minimum effective rate for saturated soils varies with $\kappa_{a,\min}$, which reflects distance from the soil surface (see Fig 2a). The value of this parameter is likely to be lower in field conditions than for experimental cores. The rest of the mineral soils exhibit peak decomposition over narrow range of matric potential. The peak for the latter generally occurs at moisture level wetter than field capacity. [Compression of the mineral soils studied by \(Franzluebbers, 1999\)](#) lowered the matric potential at which peak rate occurs. This is to be expected as compression reduces the pore sizes thereby decreasing the matric potential needed to drain the pores.

Application of the proposed model requires availability of water retention characteristic, which may pose a practical limitation in cases when water retention data cannot be readily acquired. Availability of only a handful datasets that we could use for testing the proposed model, despite the fact that decomposition

Deleted: ¶

Deleted: and Conclusions

Deleted: in the

Deleted: Compression of the mineral soils studied by (Franzluebbers, 1999)

Deleted: 4.1 Implications ¶

experiments at varying moisture statuses have been done numerous times, is a clear evidence of this challenge. As a stopgap measure, it is possible to use pedotransfer functions to infer SWC parameters based on routinely measured soil characteristics such as texture, bulk density and organic matter content (Vereecken et al., 1989; Schaap et al., 2011; Van Looy et al., 2017). The application of pedotransfer 5 functions in predicting moisture sensitivity (Eq. 12) is illustrated in Fig 11. The SWC parameters of each class were generated by the ROSETTA pedotransfer model, using class-average sand-, silt-, clay-, and SOM- content as well as bulk density in the model database (Schaap et al., 2011). As in Fig 5, two values of the parameter $\kappa_{a,\min}$ (0.2, and 0.8) were tested and the results are reported as functions of matric potential and relative moisture saturation. These curves clearly show textural effects on SOC dynamics.

10 The coarse textured soils (Sand and Loamy Sand) exhibit optimal respiration rate over a narrow range of matric potential that exceeds field capacity. While fine textured soils (Sandy Clay, Silt Clay, and Clay) exhibit broader matric potential range of optimal respiration rate, which is on the order of -1000 kPa to -100 kPa. In terms of effective saturation, the parameter $\kappa_{a,\min}$ plays the most significant role in determining the optimal saturation level. At $\kappa_{a,\min} = 0.2$, the value that was used for testing the model 15 against respiration data, the optimal effective saturation is approximately equal to 0.6. Other factors related to soil texture and structure, including mineralogy, surface area, and aggregation, are not accounted for in these moisture sensitivity curves.

Deleted:

5. Summary and Conclusions

Knowledge of controls on soil C dynamics has improved in recent years and the focus has switched from 20 predominantly molecular level controls on SOM decomposition/stability, to a broader recognition that environmental and physical conditions are more important controls on persistence of SOM. While the influence of temperature on SOM decomposition has received considerable attention, water remains the primary variable that confounds our ability to predict how soils in all climate zones will respond to perturbations both human-induced or naturally caused (Wieder et al., 2017). This model provides a first 25 step to bridging that gap (Kleber, 2010; Schmidt et al., 2011). The model has been applied to a wide range

Deleted: (Wieder et al., 2017). This model provides a first step to bridging that gap (Kleber, 2010; Schmidt et al., 2011).

of soil types highlighting the critical but underrepresented role that soil structure and water play. Results shown in Fig 5 suggest that peat soils, once drained below a threshold, are prone to rapid loss of SOC over wide range of water potential, as their bimodal pore size distribution allows them to retain sufficient moisture to promote microbial activity. The effect of warming on increasing microbial activity and rapid

5 C loss from cold high-altitude and high-latitude environments has received considerable attention in recent years ([Wieder et al., 2017](#)). SOM in these regions has been protected in part by anoxic conditions. The model proposed here suggests these soils are prone to accelerated loss of SOM due to the extended water potential range for peak decomposition afforded to them by virtue of their pore-structure. This hypothesis has yet to be tested ([Ise et al., 2008](#)).

10 The above observations also show the importance of dynamics of the physical structure of soils (e.g., tillage or slaking) in regulating SOM dynamics. For example, this model suggests that disturbance of aggregated soils initially promotes rapid mineralization by widening the pore size distribution. This mechanism is in addition to the oft-credited liberation of SOM protected inside soil aggregates. However, with repeated wetting-drying cycles the soil structure is restored to its pre-tillage state by slaking of

15 aggregates or reconsolidation by capillary forces ([Ghezzehei and Or, 2000](#); [Liu et al., 2014](#); [Or et al., 2000](#)). Therefore rapid loss of C in tilled soils is likely to be short-lived. If true, this self-limiting phenomenon is likely to have had a beneficial effect in pre-industrial agriculture, when crop nutrition was derived by recycling of SOM. High demand for nutrients during the early season is matched by rapid mineralization, while a slowdown later in the season protects SOM for subsequent seasons. To address

20 these effects of soil structure dynamics, it is important to incorporate the effect of soil structure in SWC.

The assumptions underlying the proposed model need to be tested and evaluated for wide range of soil environments. It is likely that sensitivity to water potential varies across soil types and the specific microbial communities. Therefore, variations of the slope of the water potential sensitivity curve λ across soil types and environments needs to be evaluated. Contribution of salinity to total water potential is not

25 accounted for here. Provided that total solute concentration remains constant, it is possible estimate the

dissolved fraction and its osmotic potential using sorption-desorption isotherms. However, in soils that regularly receive considerable salt inputs (e.g., saline irrigation water, fertilizers, atmospheric depositions), complete solute balance consideration is necessary.

In summary, the proposed model opens a new way of interrogating the effect of soil structure, structural dynamics and hydrologic processes on SOM dynamics. It is ~~a~~ particularly valuable tool that can support formulation of testable and quantitative hypotheses. With proper calibration and testing, this model has the potential of filling much needed coupling between biogeochemical cycling and soil hydrology over wide range of temporal and spatial scales.

Deleted: 

Tables

Table 1.

Study	Arnold	Don	Franzluebbers	Miller
Number of soil types	9	1	15 x 2	1
Water content levels	5	5	8	4
CO₂ efflux measurements	11	100?	3	1
Incubation duration (days)	395	1	24	110
Incubation temperature °C	20	21	25	lab
SWC type	Bimodal	Unimodal	Unimodal	Bimodal

References

Angert, A., Yakir, D., Rodeghiero, M., Preisler, Y., Davidson, E. A. and Weiner, T.: Using O₂ to study the relationships between soil CO₂ efflux and soil respiration, *Biogeosciences*, 12(7), 2089–2099, doi:10.5194/bg-12-2089-2015, 2015.

5 Aravena, J. E., Berli, M., Ruiz, S., Suárez, F., Ghezzehei, T. A. and Tyler, S. W.: Quantifying coupled deformation and water flow in the rhizosphere using X-ray microtomography and numerical simulations, *Plant Soil*, 376(1-2), 95–110, doi:10.1007/s11104-013-1946-z, 2013.

Arnold, C., Ghezzehei, T. A. and Berhe, A. A.: Decomposition of distinct organic matter pools is regulated by moisture status in structured wetland soils, *Soil Biol Biochem*, 10 doi:10.1016/j.soilbio.2014.10.029, 2015.

Birch, H. F., The effect of soil drying on humus decomposition and nitrogen availability *Plant and Soil* 10:9-31, 1958.

Carbone, M. S., Still, C. J., Ambrose, A. R., Dawson, T. E., Williams, A. P., Boot, C. M., Schaeffer, S. M. and Schimel, J. P.: Seasonal and episodic moisture controls on plant and microbial contributions to 15 soil respiration, *Oecologia*, 167(1), 265–278, doi:10.1007/s00442-011-1975-3, 2011.

Chowdhury, N., Marschner, P. and Burns, R.: Response of microbial activity and community structure to decreasing soil osmotic and matric potential, *Plant Soil*, 344(1-2), 241–254, doi:10.1007/s11104-011-0743-9, 2011a.

Chowdhury, N., Marschner, P. and Burns, R. G.: Soil microbial activity and community composition: 20 Impact of changes in matric and osmotic potential, *Soil Biol Biochem* 43(6), 1229–1236, doi:10.1016/j.soilbio.2011.02.012, 2011b.

Coleman, K. and Jenkinson, D. S.: RothC-26.3 - A Model for the turnover of carbon in soil, in *Evaluation of Soil Organic Matter Models*, pp. 237–246, Springer, Berlin, Heidelberg, Berlin, Heidelberg, 1996.

Csonka, L. N.: Physiological and genetic responses of bacteria to osmotic stress, *Microbiol. Rev.*, 53(1), 25 121–147, 1989.

Davidson, E. A., Samanta, S., Caramori, S. S. and Savage, K.: The Dual Arrhenius and Michaelis–Menten kinetics model for decomposition of soil organic matter at hourly to seasonal time scales, *Global Change Biology*, 18(1), 371–384, doi:10.1111/j.1365-2486.2011.02546.x, 2012.

Durner, W.: Hydraulic Conductivity Estimation for Soils with Heterogeneous Pore Structure, *Water Resour Res*, 30(2), 211–223, 1994.

Elzhov, T. V., Mullen, K. M., Spiess, A.-N. and Ben Bolker: minpack.lm: R Interface to the Levenberg–Marquardt Nonlinear Least-Squares Algorithm Found in MINPACK, Plus Support for Bounds, R Foundation for Statistical Computing, 2016.

Finsterle, S. and Persoff, P.: Determining permeability of tight rock samples using inverse modeling, 35 *Water Resour Res*, 33(8), 1803–1811, doi:10.1029/97WR01200, 1997.

Franzluebbers, A. J.: Microbial activity in response to water-filled pore space of variably eroded southern Piedmont soils, *Applied Soil Ecology*, 11, 91–101, 1999.

Deleted: 

Ghezzehei, T. A.: Dynamics of soil aggregate coalescence governed by capillary and rheological processes,, 36(2), 367–379, 2000.

Ghezzehei, T. A. and Or, D.: Dynamics of soil aggregate coalescence governed by capillary and rheological processes, Water Resour Res, 36(2), 367–379, doi:10.1029/1999WR900316, 2000.

5 Grajek, W. and Gervais, P.: Influence of water activity on the enzyme biosynthesis and enzyme activities produced by *Trichoderma viride* TS in solid-state fermentation, Enzyme and Microbial Technology, 9(11), 658–662, doi:10.1016/0141-0229(87)90123-2, 1987.

Harris, R. F.: Effect of Water Potential on Microbial Growth and Activity, Water Potential Relations in Soil Microbiology, SSSA Special publication, 23–95, doi:10.2136/sssaspecpub9.c2, 1981.

10 Hillel, D.: Environmental soil physics, Academic Press, , 1998.

Iden, S. C., and W. Durner, Comment on “Simple consistent models for water retention and hydraulic conductivity in the complete moisture range” by A. Peters, Water Resour. Res., 50, 7530–7534, 2014.

Ise, T., Dunn, A. L., Wofsy, S. C. and Moorcroft, P. R.: High sensitivity of peat decomposition to climate change through water-table feedback, NATURE GEOSCIENCE, 1(11), 763–766, doi:10.1038/ngeo331, 15 2008.

Kleber, M.: Response to the Opinion paper by Margit von Lützow and Ingrid Kögel-Knabner on“What is recalcitrant soil organic matter?” by Markus Kleber, Environmental Chemistry, 7(4), 336–337, 2010.

Kredics, L., Antal, Z. and Manczinger, L.: Influence of Water Potential on Growth, Enzyme Secretion and In Vitro Enzyme Activities of *Trichoderma harzianum* at Different Temperatures, Curr Microbiol, 20 40(5), 310–314, doi:10.1007/s00249910062, 2000.

Linn, D. M. and Doran, J. W.: Effect of Water-Filled Pore Space on Carbon Dioxide and Nitrous Oxide Production in Tilled and Nontilled Soils 1, Soil Sci Soc Am J Soil Sci Soc Am J, 48(6), 1267–1272, doi:10.2136/sssaj1984.03615995004800060013x, 1984.

Liu, X., Lu, Sen, Horton, R. and Ren, T.: In Situ Monitoring of Soil Bulk Density with a Thermo-TDR Sensor, Soil Sci Soc Am J Soil Sci Soc Am J, 78(2), 400–407, doi:10.2136/sssaj2013.07.0278, 2014.

Manzoni, S. and Katul, G.: Invariant soil water potential at zero microbial respiration explained by hydrological discontinuity in dry soils, Geophys Res Lett, 41(20), 7151–7158, doi:10.1002/2014GL061467, 2014.

Miller, A. E., Schimel, J. P., Meixner, T., Sickman, J. O. and Melack, J. M.: Episodic rewetting enhances 30 carbon and nitrogen release from chaparral soils, Soil Biol Biochem Soil Biol Biochem, 37(12), 2195–2204, doi:10.1016/j.soilbio.2005.03.021, 2005.

Moldrup, P., Olesen, T., Yoshikawa, S., Komatsu, T. and Rolston, D. E.: Three-Porosity Model for Predicting the Gas Diffusion Coefficient in Undisturbed Soil, Soil Sci Soc Am J, 68(3), 750–759, doi:10.2136/sssaj2004.7500, 2004.

35 Monard, C., Mchergui, C., Nunan, N., Martin-Laurent, F. and Vieuillé-Gonod, L.: Impact of soil matric potential on the fine-scale spatial distribution and activity of specific microbial degrader communities, Fems Microbiol Ecol, 81(3), 673–683, doi:10.1111/j.1574-6941.2012.01398.x, 2012.

Deleted: sssaspecialpubl(waterpotentialr),

Deleted: ..

Manzoni, S., F. Moyano, T. Kätterer, and J. Schimel. 2016. Modeling coupled enzymatic and solute transport controls on decomposition in drying soils. *Soil Biology and Biochemistry* 95:275-287.

Moyano, F. E., Manzoni, S. and Chenu, C.: Responses of soil heterotrophic respiration to moisture availability: An exploration of processes and models, *Soil Biol Biochem*, 59, 72–85, doi:10.1016/j.soilbio.2013.01.002, 2013.

Moyano, F. E., Vasilyeva, N., Bouckaert, L., Cook, F., Craine, J., ~~Yuste, J.C.~~, Don, A., Epron, D., Formanek, P., Franzluebbers, A., Ilstedt, U., Kätterer, T., Orchard, V., Reichstein, M., Rey, A., Ruamps, L., Subke, J. A., Thomsen, I. K. and CHENU, C.: The moisture response of soil heterotrophic respiration: interaction with soil properties, *Biogeosciences*, 9(3), 1173–1182, doi:10.5194/bg-9-1173-2012, 2012.

10 Moyano, F. E., Vasi-lyeva, N., and Menichetti, L.: Diffusion based modelling of temperature and moisture interactive effects on carbon fluxes of mineral soils, *Biogeosciences Discuss.*, <https://doi.org/10.5194/bg-2018-95>, in review, 2018.

Or, D. and Tuller, M.: Liquid retention and interfacial area in variably saturated porous media: Upscaling from single-pore to sample-scale model, *Water Resour Res*, 35(12), 3591–3605, 1999.

15 Or, D., Leij, F. J., Snyder, V. and Ghezzehei, T. A.: Stochastic model for posttillage soil pore space evolution, *Water Resour Res*, 36(7), 1641–1652, 2000.

Parton, W. J., Hartman, M., Ojima, D. and Schimel, D.: DAYCENT and its land surface submodel: description and testing, *Global and Planetary Change*, 19(1-4), 35–48, doi:10.1016/S0921-8181(98)00040-X, 1998.

20 Peters, A. (2013), Simple consistent models for water retention and hydraulic conductivity in the complete moisture range, *Water Resour. Res.*, 49, 6765–6780.

Pisani, L.: Simple Expression for the Tortuosity of Porous Media, *Transport Porous Med Transport Porous Med*, 88(2), 193–203, doi:10.1007/s11242-011-9734-9, 2011.

R Core Team: R: A Language and Environment for Statistical Computing, R Foundation for Statistical Computing, Vienna, Austria. 2017.

25 Ruiz, S., Or, D. and Schymanski, S. J.: Soil Penetration by Earthworms and Plant Roots—Mechanical Energetics of Bioturbation of Compacted Soils, edited by R. Balestrini, *PLoS ONE*, 10(6), e0128914, doi:10.1371/journal.pone.0128914, 2015.

30 Schaa p, M. G., Leij, F. J. and van Genuchten, M. T.: ROSETTA: A computer program for estimating soil hydraulic parameters with hierarchical pedotransfer functions, *J Hydrol J Hydrol*, 251(3-4), 163–176, doi:10.1016/S0022-1694(01)00466-8, 2001.

Schindler, U., Durner, W., Unold, von, G., Mueller, L. and Wieland, R.: The evaporation method: Extending the measurement range of soil hydraulic properties using the air-entry pressure of the ceramic cup, *Journal of Plant Nutrition and Soil Science*, 173(4), 563–572, doi:10.1002/jpln.200900201, 2010.

35 Schjønning, P., Thomsen, I. K., Moldrup, P. and Christensen, B. T.: Linking Soil Microbial Activity to Water- and Air-Phase Contents and Diffusivities, *Soil Sci Soc Am J*, 67(1), 156–165, doi:10.2136/sssaj2003.1560, 2003.

Schjønning, P., Thomsen, I. K., Petersen, S. O., Kristensen, K. and Christensen, B. T.: Relating soil microbial activity to water content and tillage-induced differences in soil structure, *Geoderma* **163**(3-4), 256–264, doi:10.1016/j.geoderma.2011.04.022, 2011.

Schmidt, M. W. I., Torn, M. S., Abiven, S., Dittmar, T., Guggenberger, G., Janssens, I. A., Kleber, M., Kogel-Knabner, I., Lehmann, J., Manning, D. A. C., Nannipieri, P., Rasse, D. P., Weiner, S. and Trumbore, S. E.: Persistence of soil organic matter as an ecosystem property, *Nature*, **478**(7367), 49–56, doi:10.1038/nature10386, 2011.

Scott, N. A., Cole, C. V., Elliott, E. T. and Huffman, S. A.: Soil Textural Control on Decomposition and Soil Organic Matter Dynamics, *Soil Sci Soc Am J* **60**(4), 1102–1109, doi:10.2136/sssaj1996.03615995006000040020x, 1996.

Sierra, C. A., Malghani, S. and Loescher, H. W.: Interactions among temperature, moisture, and oxygen concentrations in controlling decomposition rates in a boreal forest soil, *Biogeosciences*, **14**(3), 703–710, doi:10.5194/bg-14-703-2017, 2017.

Skopp, J., Jawson, M. D. and Doran, J. W.: Steady-State Aerobic Microbial Activity as a Function of Soil Water Content, *Soil Sci Soc Am J* **54**(6), 1619–1625, doi:10.2136/sssaj1990.03615995005400060018x, 1990.

Skujins, J. J. and McLaren, A. D.: Enzyme Reaction Rates at Limited Water Activities, *Science*, **158**(3808), 1569–1570, doi:10.1126/science.158.3808.1569, 1967.

Stark, J. M. and Firestone, M. K.: Mechanisms for soil moisture effects on activity of nitrifying bacteria, *Applied Environmental Microbiology*, **61**(1), 218–221, 1995.

Sulman, B. N., Desai, A. R., Schroeder, N. M., Ricciuto, D., Barr, A., Richardson, A. D., Flanagan, L. B., Lafleur, P. M., Tian, H., Chen, G., Grant, R. F., Poulter, B., Verbeeck, H., Ciais, P., Ringeval, B., Baker, I. T., Schaefer, K., Luo, Y. and Weng, E.: Impact of hydrological variations on modeling of peatland CO₂ fluxes: Results from the North American Carbon Program site synthesis, *Journal of Geophysical Research: Biogeosciences*, **117**(G1), 37, doi:10.1029/2011JG001862, 2012.

Šimůnek, J., van Genuchten, M. T. and Šejna, M.: Recent Developments and Applications of the HYDRUS Computer Software Packages, *Vadose Zone J*, **15**(7), 0, doi:10.2136/vzj2016.04.0033, 2016.

[Tang, J. Y., and W. J. Riley. A total quasi-steady-state formulation of substrate uptake kinetics in complex networks and an example application to microbial litter decomposition. Biogeosciences 10:8329-8351, 2013.](#)

Tecon, R. and Or, D.: Biophysical processes supporting the diversity of microbial life in soil, *FEMS Microbiol Rev*, **41**(5), 599–623, doi:10.1093/femsre/fux039, 2017.

Thomsen, I. K., Schjønning, P., Jensen, B., Kristensen, K. and Christensen, B. T.: Turnover of organic matter in differently textured soils, *Geoderma*, **89**(3-4), 199–218, doi:10.1016/S0016-7061(98)00084-6, 1999.

Tresner, H. D. and Hayes, J. A.: Sodium Chloride Tolerance of Terrestrial Fungi, *Appl Environ Microb*, **22**(2), 210–213, 1971.

van Genuchten, M. T.: A Closed-form Equation for Predicting the Hydraulic Conductivity of Unsaturated Soils1, *Soil Sci Soc Am J Soil Sci Soc Am J*, 44(5), 892–898, doi:10.2136/sssaj1980.03615995004400050002x, 1980.

5 [Van Looy, K., Bouma, J., Herbst, M., Koestel, J., Minasny, B., Mishra, U., ... Vereecken, H. \(2017\). Pedotransfer Functions in Earth System Science: Challenges and Perspectives. *Reviews of Geophysics*, 55\(4\), 1199–1256. https://doi.org/10.1002/2017RG000581](#)

Deleted: WATSON

Vereecken, H., Maes, J., Feyen, J., & Darius, P. (1989). Estimating the Soil Moisture Retention Characteristic From Texture, Bulk Density, and Carbon Content. *Soil Science*, 148(6), 389–403. Retrieved from <https://insights.ovid.com/crossref?an=00010694-198912000-00001>

10 [Watson, T. G.: Effects of Sodium Chloride on Steady-state Growth and Metabolism of *Saccharomyces cerevisiae*, *Microbiology*, 64\(1\), 91–99, doi:10.1099/00221287-64-1-91, 1970.](#)

Wickland, K. P. and Neff, J. C.: Decomposition of soil organic matter from boreal black spruce forest: environmental and chemical controls, *Biogeochemistry Biogeochemistry*, 87(1), 29–47, doi:10.1007/s10533-007-9166-3, 2007.

15 [Wieder, W. R., Hartman, M. D., Sulman, B. N., Wang, Y. P., Koven, C. D. and Bonan, G. B.: Carbon cycle confidence and uncertainty: Exploring variation among soil biogeochemical models, *Global Change Biology*, 24\(4\), 1563–1579, doi:10.1111/gcb.13979, 2017.](#)

20 [Wood, J. M.: Bacterial Osmoregulation: A Paradigm for the Study of Cellular Homeostasis, http://dx.doi.org/10.1146/annurev-micro-090110-102815, 65\(1\), 215–238, doi:10.1146/annurev-micro-090110-102815, 2011.](#)

25 [Yan, Z., Liu, C., Todd-Brown, K.E. et al. Pore-scale investigation on the response of heterotrophic respiration to moisture conditions in heterogeneous soils. *Biogeochemistry* 131: 121–134, 2016.](#)

[Yan, Z., B. Bond-Lamberty, K. E. Todd-Brown, V. L. Bailey, S. Li, C. Liu, and C. Liu. A moisture function of soil heterotrophic respiration that incorporates microscale processes. *Nature communications* 9:2562, 2018.](#)

30 [Yuste, J. C., Baldocchi, D. D., Gershenson, A., Goldstein, A., Misson, L. and WONG, S.: Microbial soil respiration and its dependency on carbon inputs, soil temperature and moisture, *Global Change Biology*, 13\(9\), 2018–2035, doi:10.1111/j.1365-2486.2007.01415.x, 2007.](#)

[Zhang, Y. and Schaap, M. G.: Weighted recalibration of the Rosetta pedotransfer model with improved estimates of hydraulic parameter distributions and summary statistics \(Rosetta3\), *J Hydrol J Hydrol*, 547, 39–53, doi:10.1016/j.jhydrol.2017.01.004, 2017.](#)

Deleted: YUSTE

Deleted: BALDOCCHI

Deleted: GERSHENSON

Deleted: GOLDSTEIN

Deleted: MISSON

Formatted: Normal, Don't adjust space between Latin and Asian text, Don't adjust space between Asian text and numbers, Tab stops: 0.39", Left + 0.78", Left + 1.17", Left + 1.56", Left + 1.94", Left + 2.33", Left + 2.72", Left + 3.11", Left + 3.5", Left + 3.89", Left + 4.28", Left + 4.67", Left

Deleted: 1

... [1]

Formatted: English (US)

Page 27: [1] Deleted

Author

▼

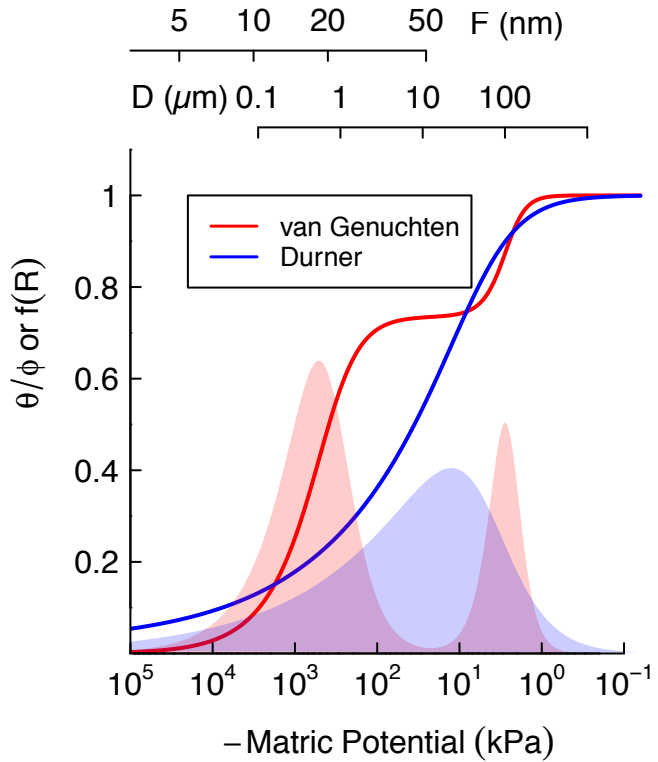


Figure 1: Schematic comparison of unimodal vs biomodal soil water characteristic (SWC) curves, represented using van Genuchten (1980) and Durner (1994) models, respectively. Shaded regions are distribution functions of effective pore throat diameter. Scales on top show the thickness of adsorbed film and pore-throat diameter corresponding to the water potentials.

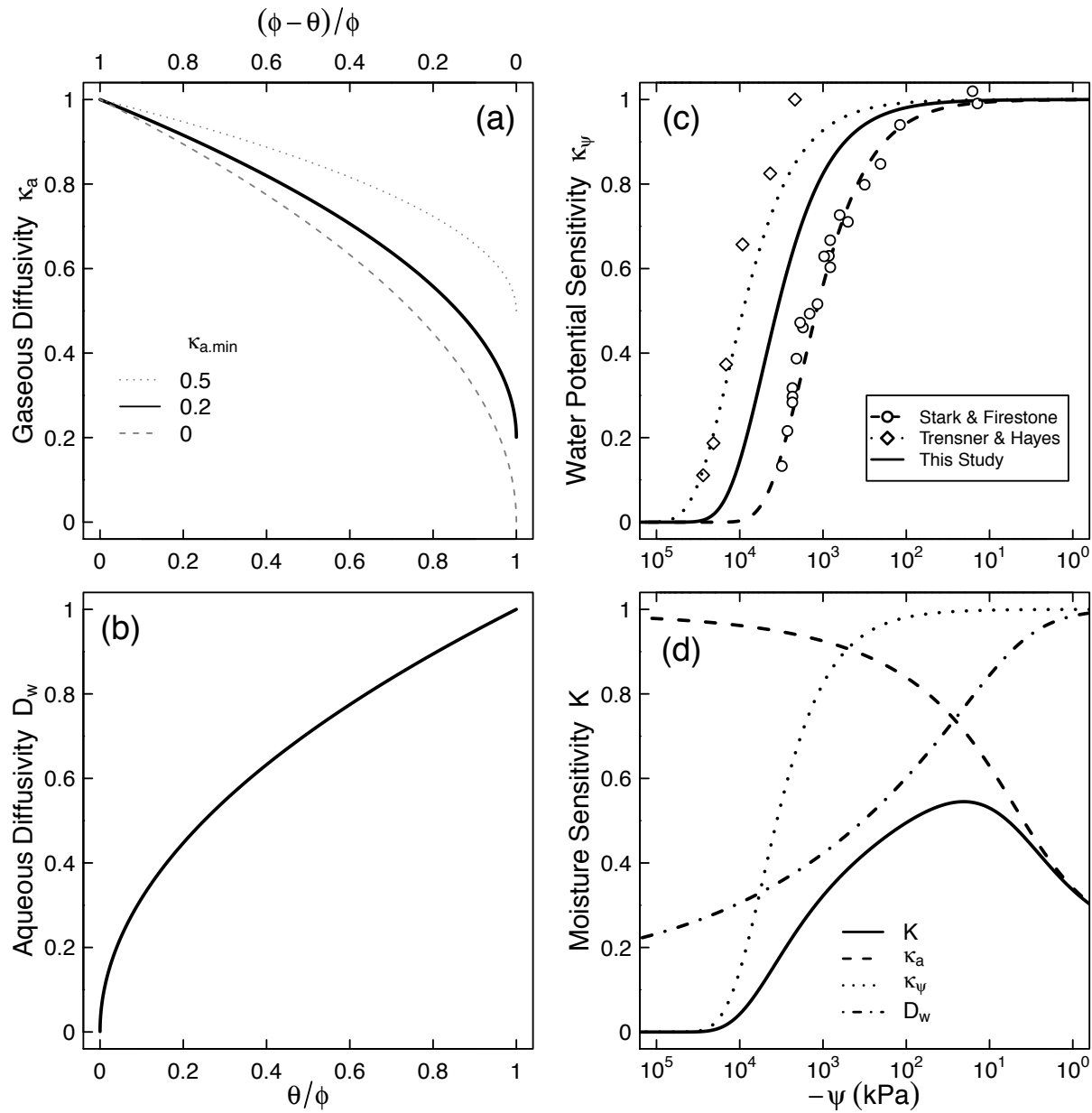


Figure 2: Relative contributions of (a) air diffusion on access to O_2 , (b) aqueous diffusion limitation on substrate access, (c) limiting effect of water potential on microbial activity, and (d) the combined effect of the three factors for a soil characterized by a unimodal SWC curve shown in Figure 1.

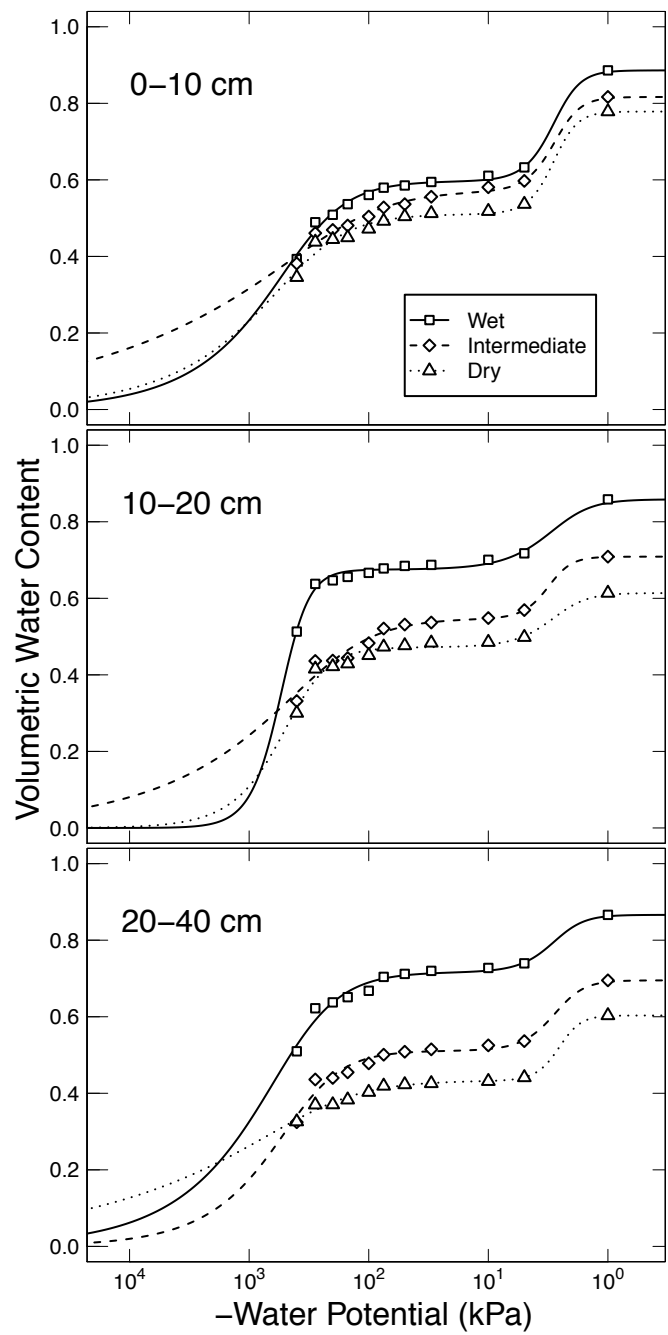


Figure 3: Water retention characteristics of meadow soils (Arnold et al, 2014) that were used to derive the relative effect of water potential on overall mineralization rate.

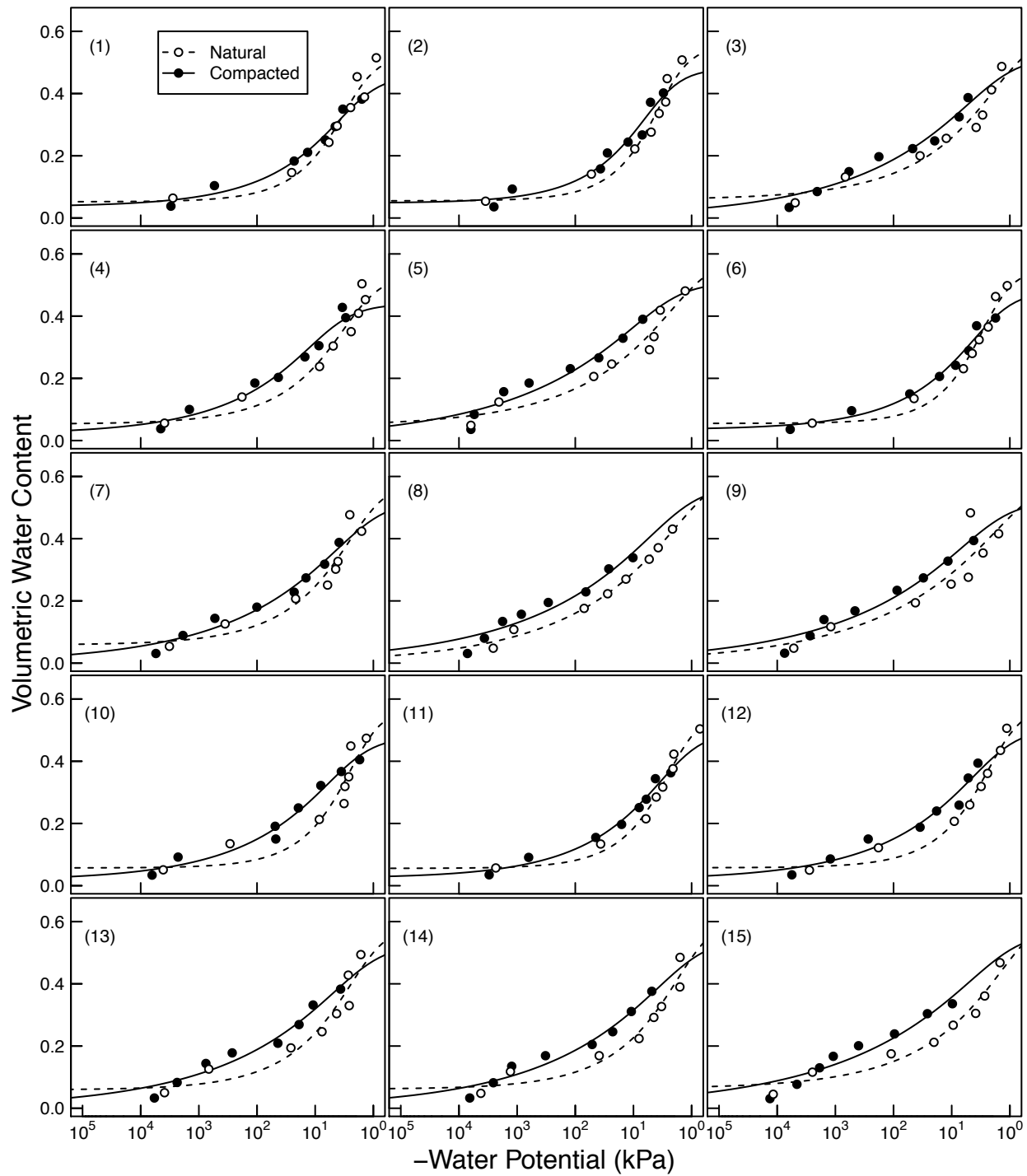


Figure 4: Soil moisture characteristics of soils analyzed by Franzluebers (1999); symbols are measured values and lines are van Genuchten model fits. The best fit n parameter are shown. Soils at natural (triangle symbol and dashed line) and compacted (circle and solid lines) state were studied.

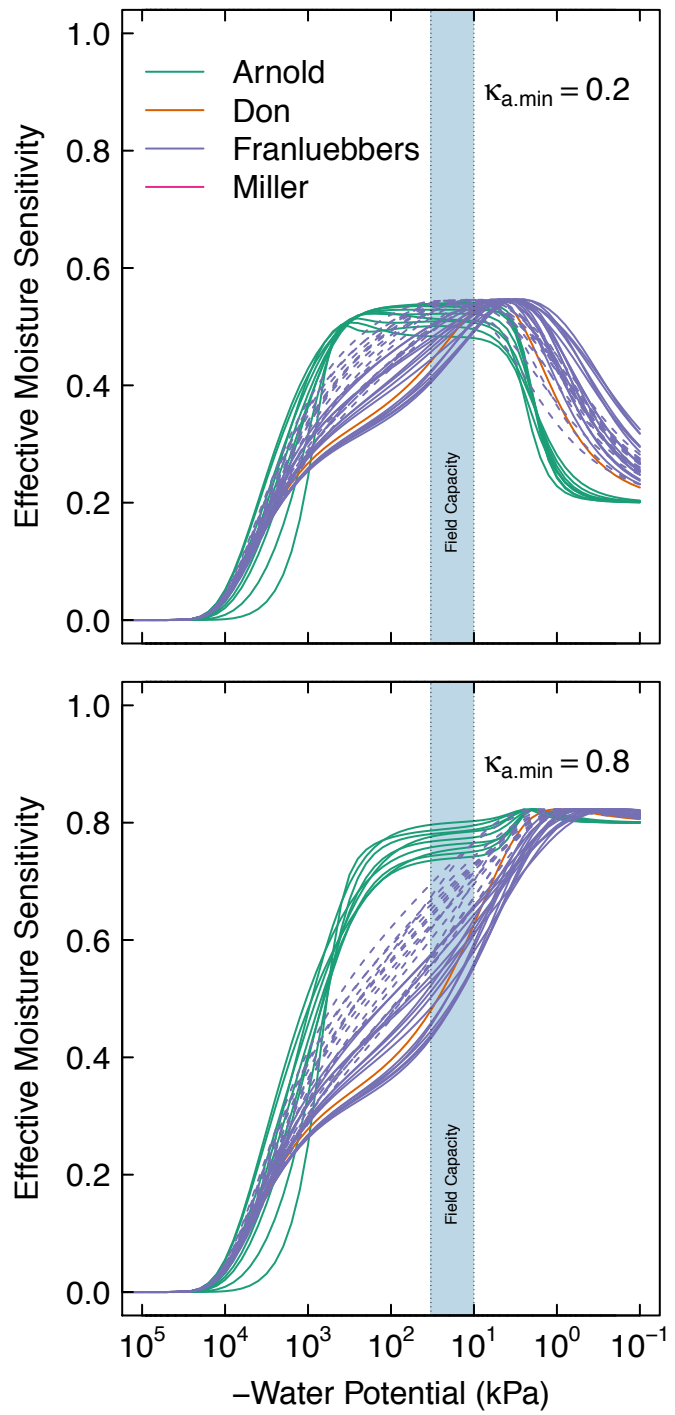


Figure 5: Effective soil moisture sensitivity functions for all the soils. These curves were calculated as illustrated in Figure 2 using $\kappa_{a,\min} = 0.8$ (top) and $\kappa_{a,\min} = 0.2$ (bottom). The shaded region ($-300 \leq \psi - 100$) denotes the typical range of field capacity.

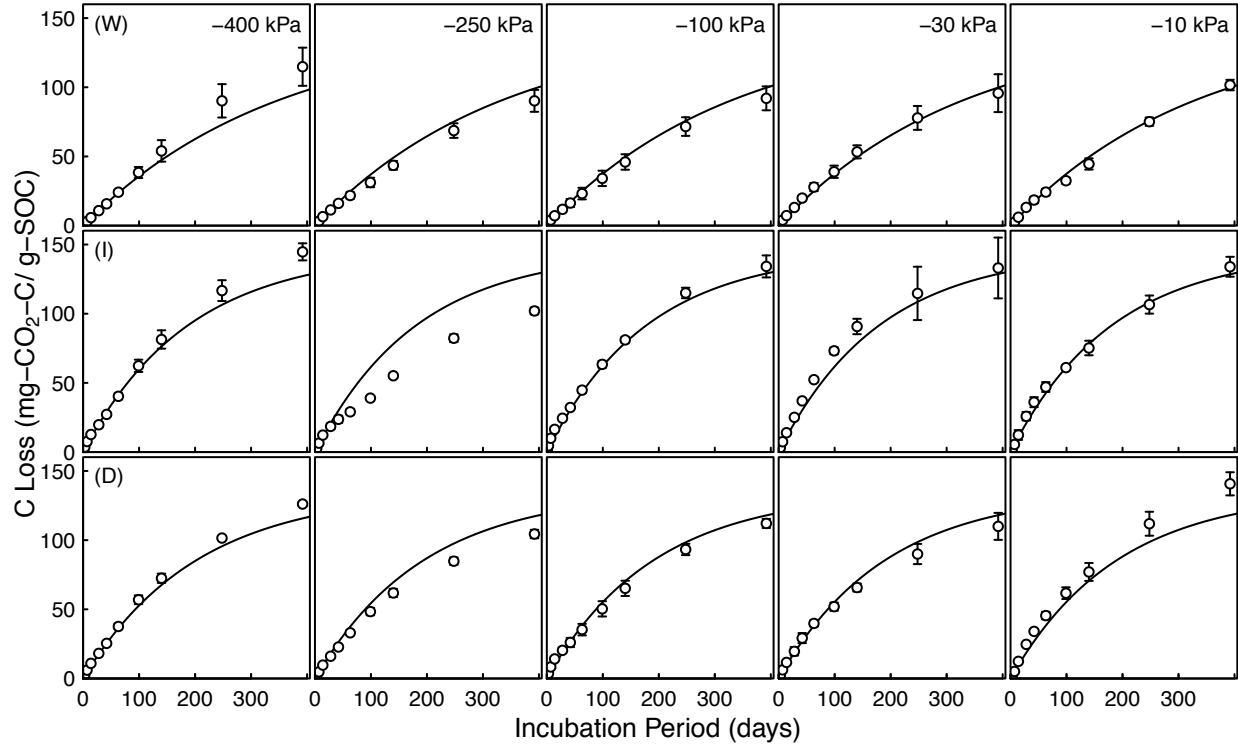


Figure 6: Evolution of CO₂ during 395 day incubation of soils collected from Dana Meadows (Yosemite National Park) from 0-10 cm depth over a wide range of water potentials. Other depths are provided in supplemental data. Soils from three hydrologic regimes are shown in the three rows: W = wet (top row), I = intermediate (middle row), and D = dry (bottom row). The columns represent equilibrium matric potential conditions.

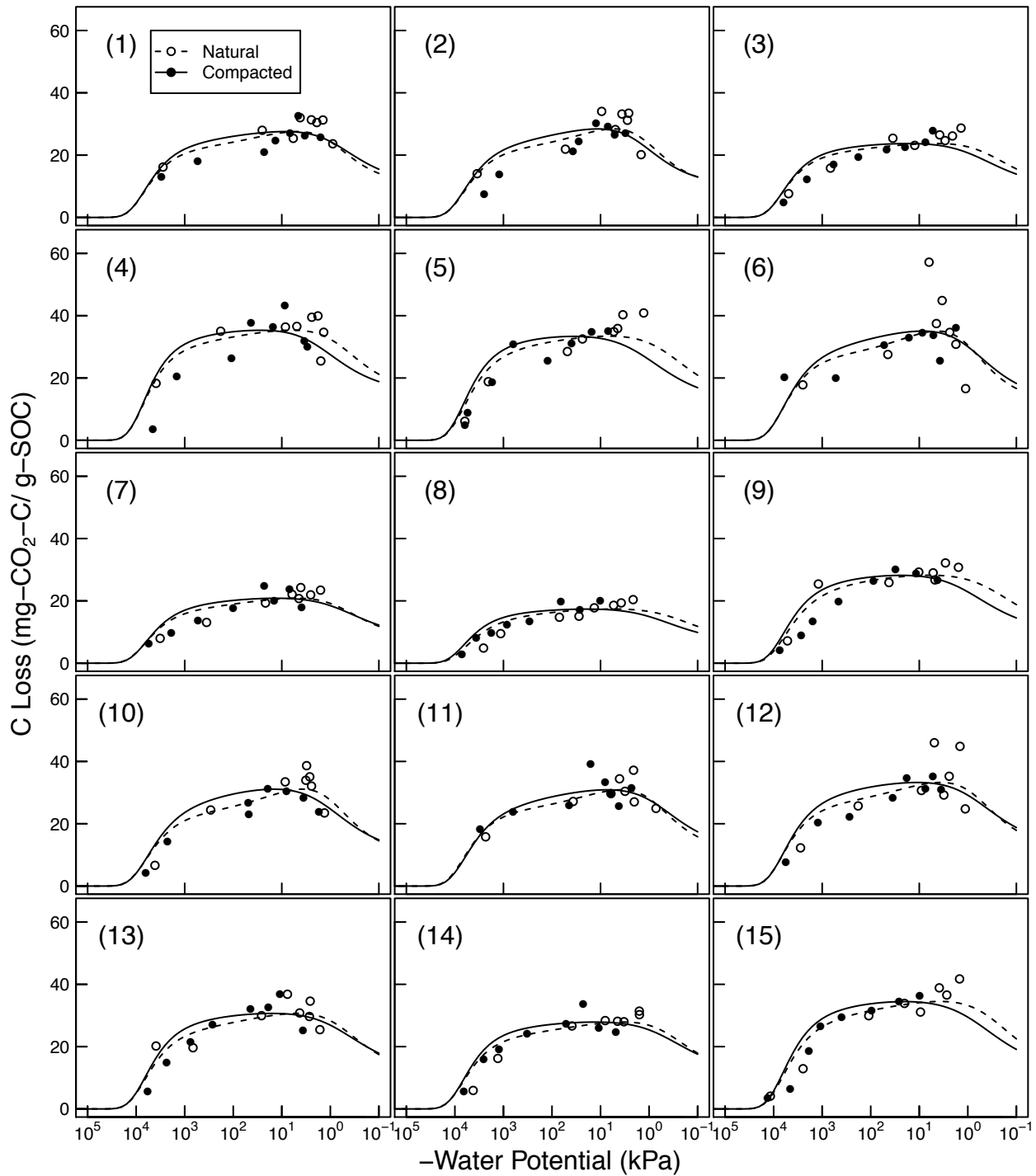


Figure 7: Comparison of total SOC loss during 24 day incubation of 15 soils analyzed by Franzluebers (1999) (at naturally settled and compressed states); symbols are measured values and lines are model simulations using van Genuchten SWC curves and decomposition parameters, C_0 and κ_0 , fitted to individually to each of the 15 soil types.

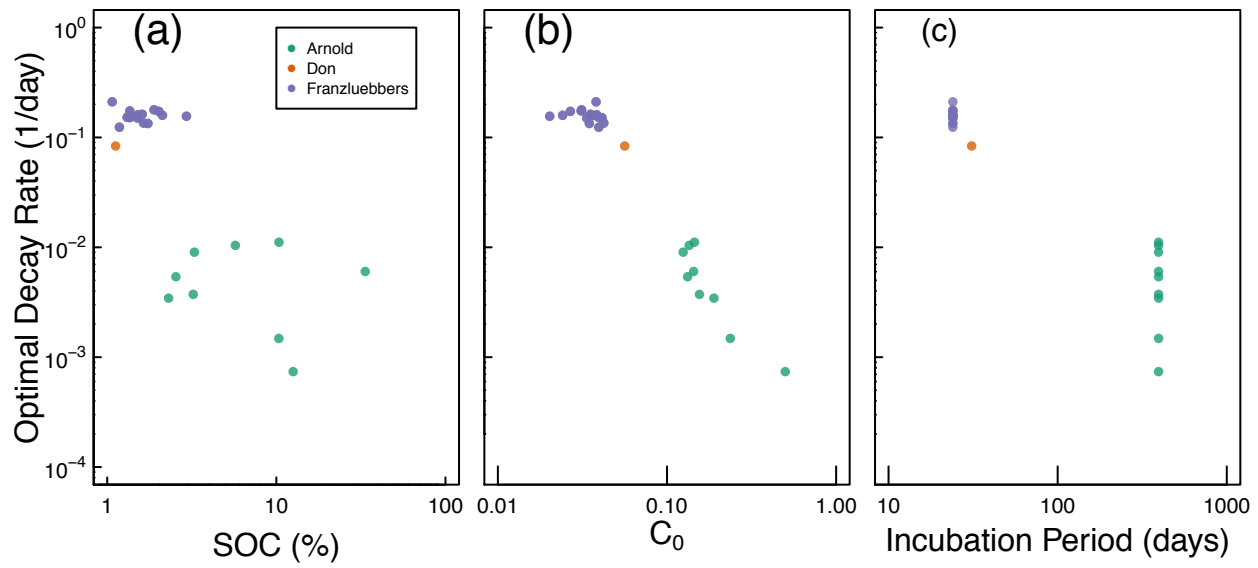


Figure 8: Relationships among fitted decomposition parameters C_0 and κ_o as well as with soil organic C content (SOC) and length of incubation period.

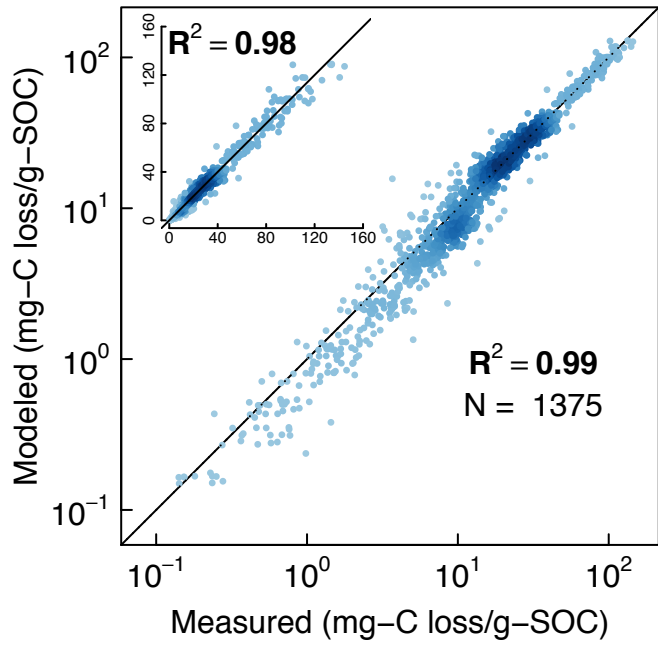


Figure 9: Comparison of model simulations with measured cumulative CO₂ evolution data from all incubation studies at steady-water content.

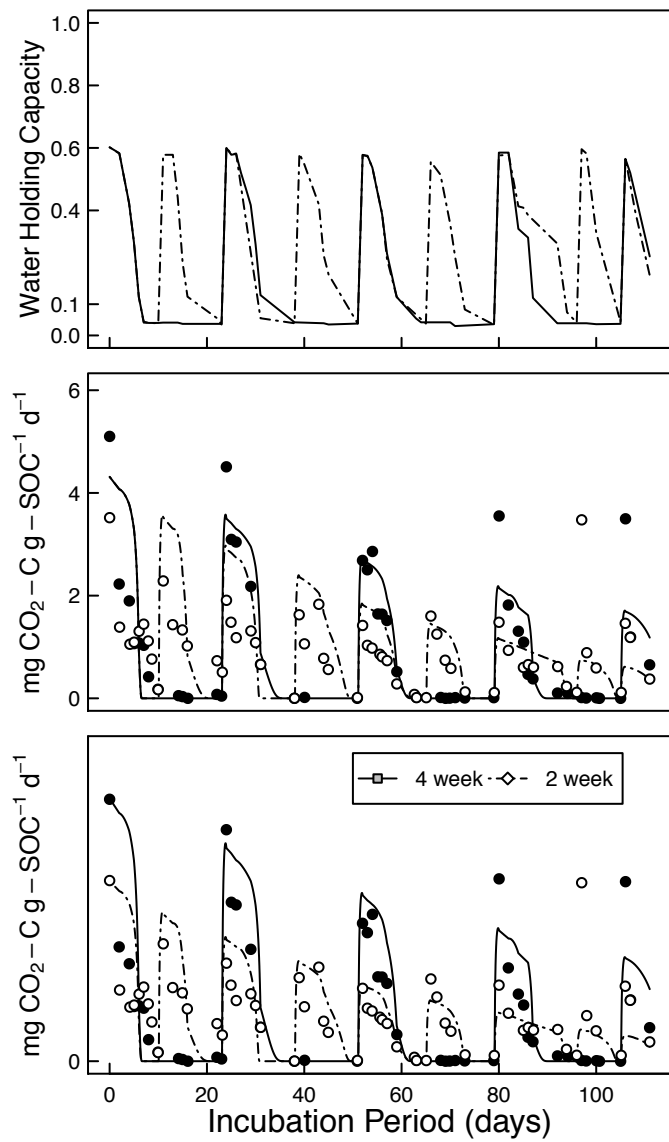


Figure 10: Comparison of measured CO_2 efflux during 2- and 4-week rewetting experiment (a) with model predicted efflux assuming (b) identical decomposition parameters for both wetting intervals and (c) separate decomposition parameters for the two wetting intervals.

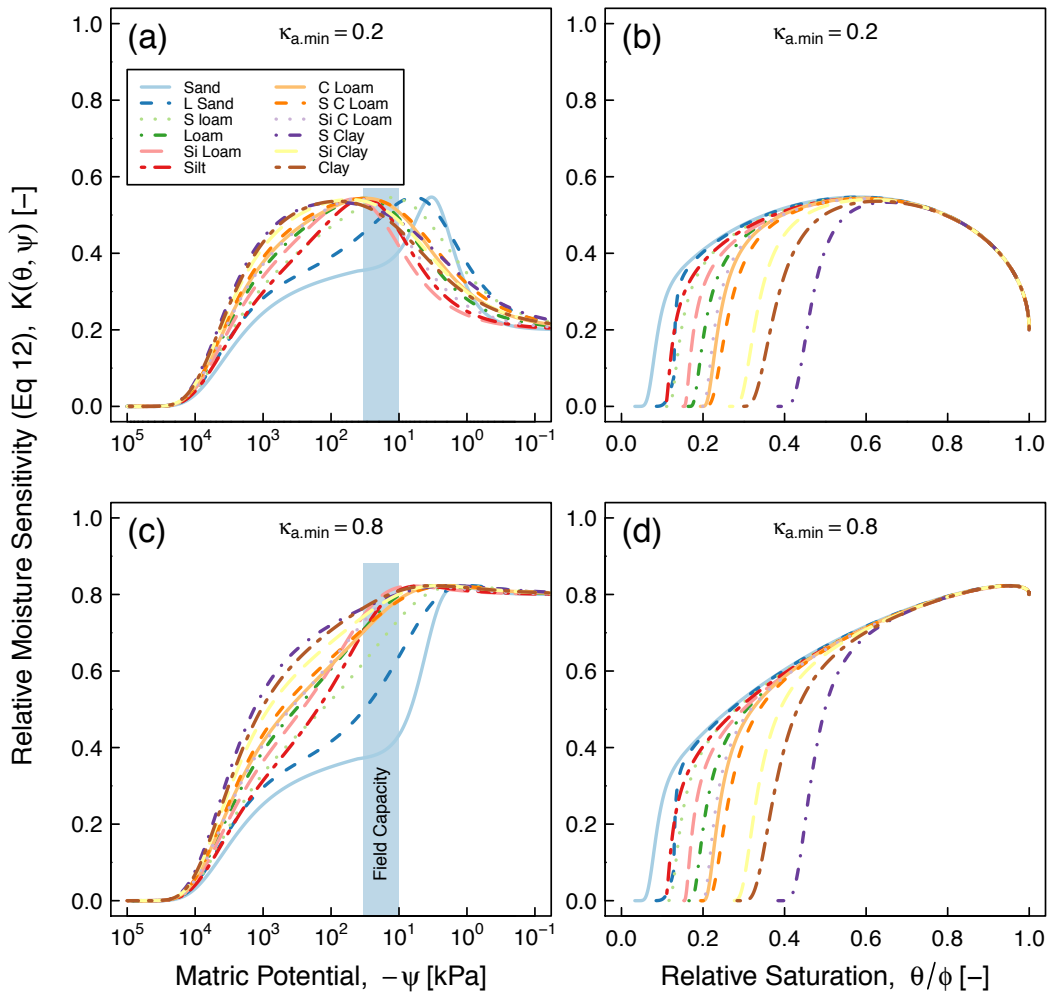


Figure 11: Textural effect on moisture sensitivity

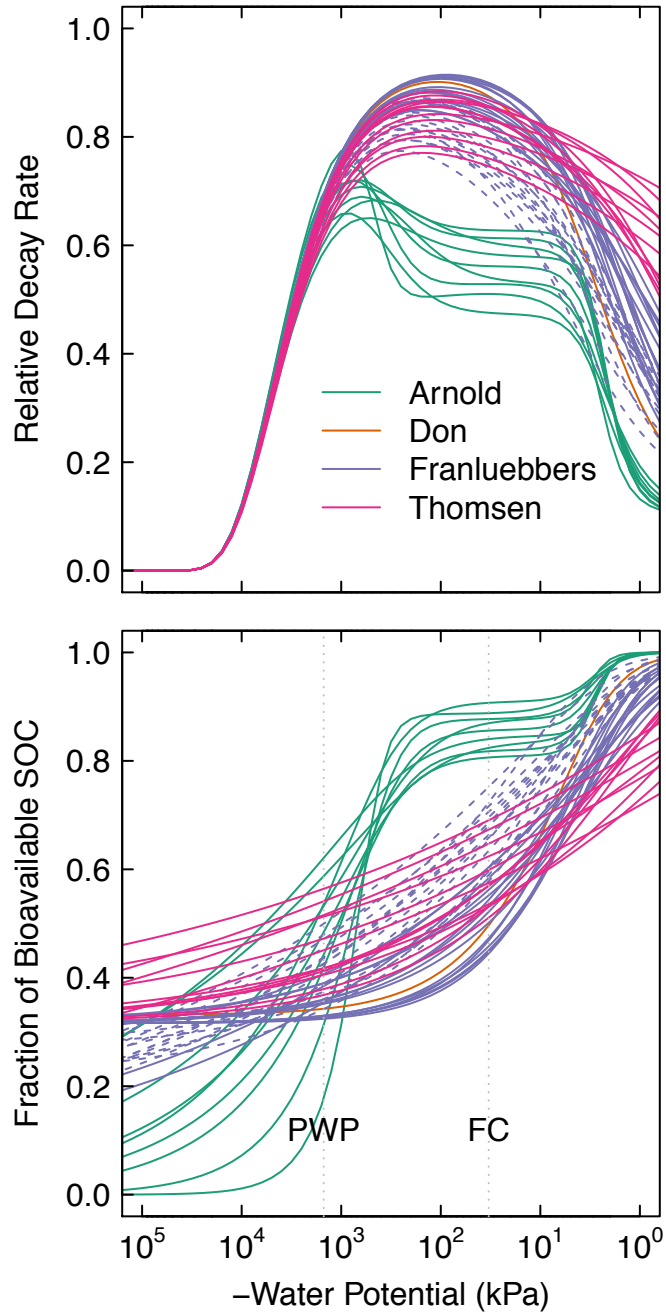


Figure A.1: Moisture-dependent, relative (dimensionless) parameters of 51 different soils: (a) decay rate and (b) fraction of bioavailable SOC. Each of the curves are entirely dependent only on the water retention characteristic of the respective soils. The dashed-lines of the Franzluebbers soils denote compressed samples. PWP = permanent wilting point ($\psi = -1500$ kPa) and FC = field capacity ($\psi = -300$ kPa)

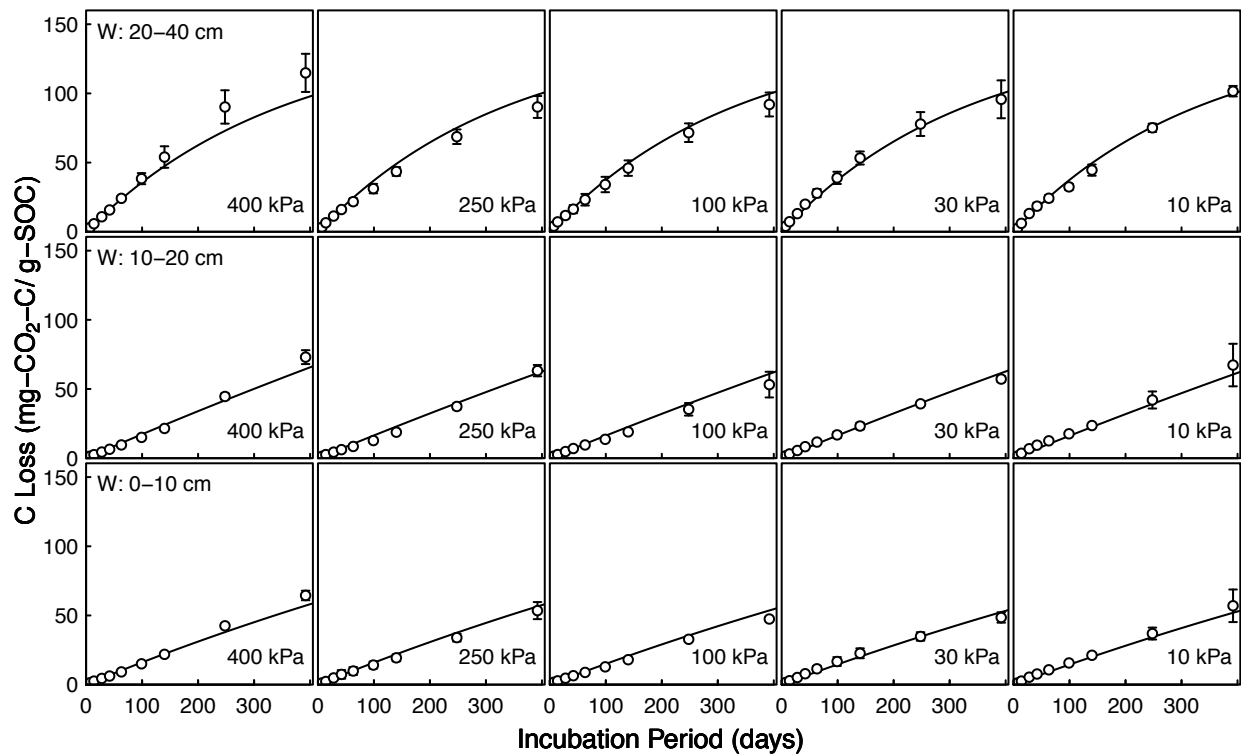


Figure A.2: (part 1/3) Decomposition experiments of Arnold et al. fitted CO_2 evolution data from 395-day incubation experiment: Part 1 wet meadow.

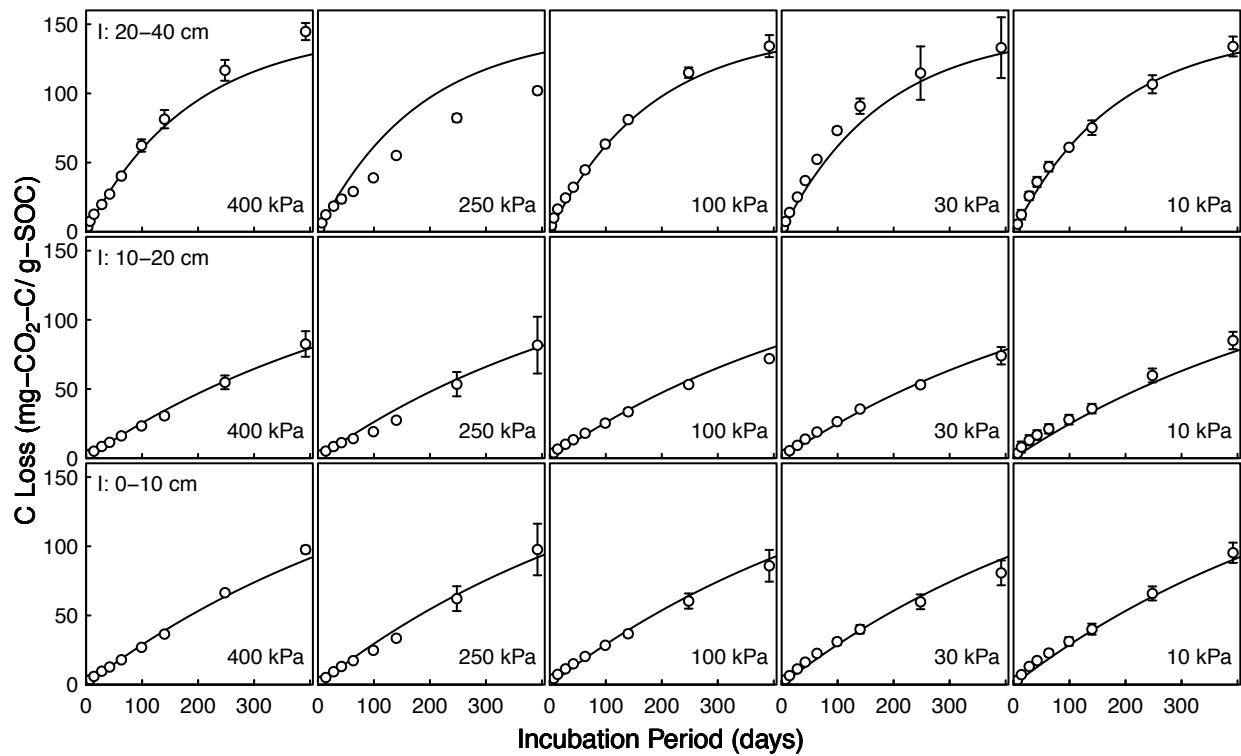


Figure A.2: (part 2/3) Decomposition experiments of Arnold et al. fitted CO₂ evolution data from 395-day incubation experiment: Part 2 intermediate meadow.

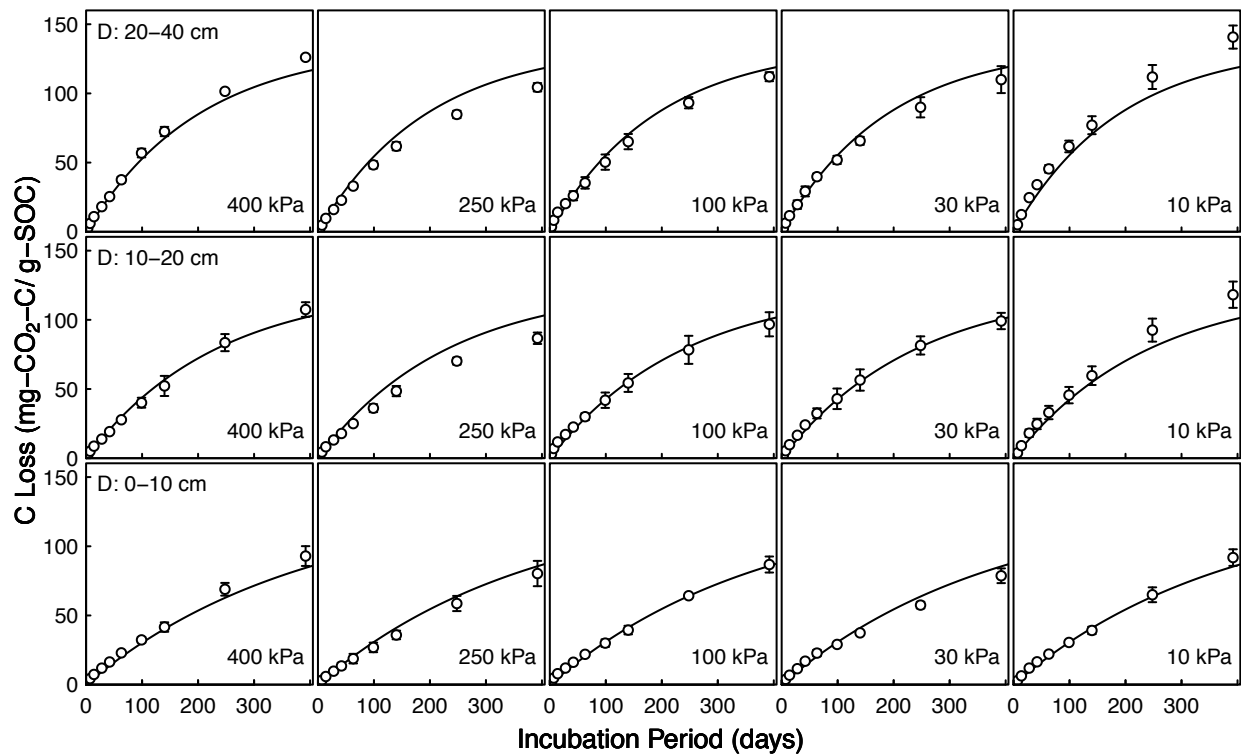


Figure A.2: (part 3/3) Decomposition experiments of Arnold et al. fitted CO₂ evolution data from 395-day incubation experiment: Part 3 dry meadow.

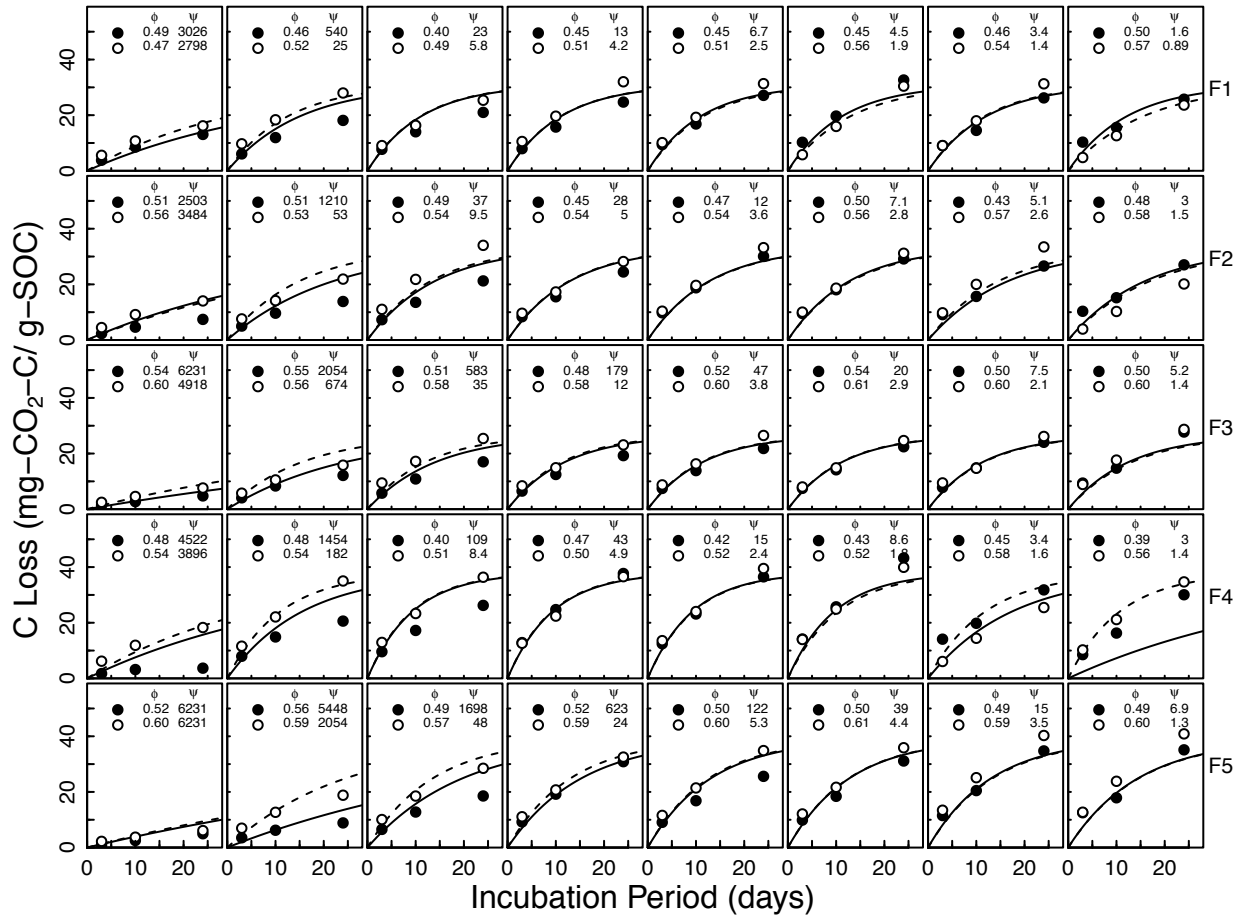


Figure A.3: (part 1/3) Decomposition experiments of Franzluebbers et al; fitted CO₂ evolution data. Fifteen different soils packed at two bulk density values incubated eight matric potential levels for 24 days. The porosity, water potential and RMSE of each sample are shown inside

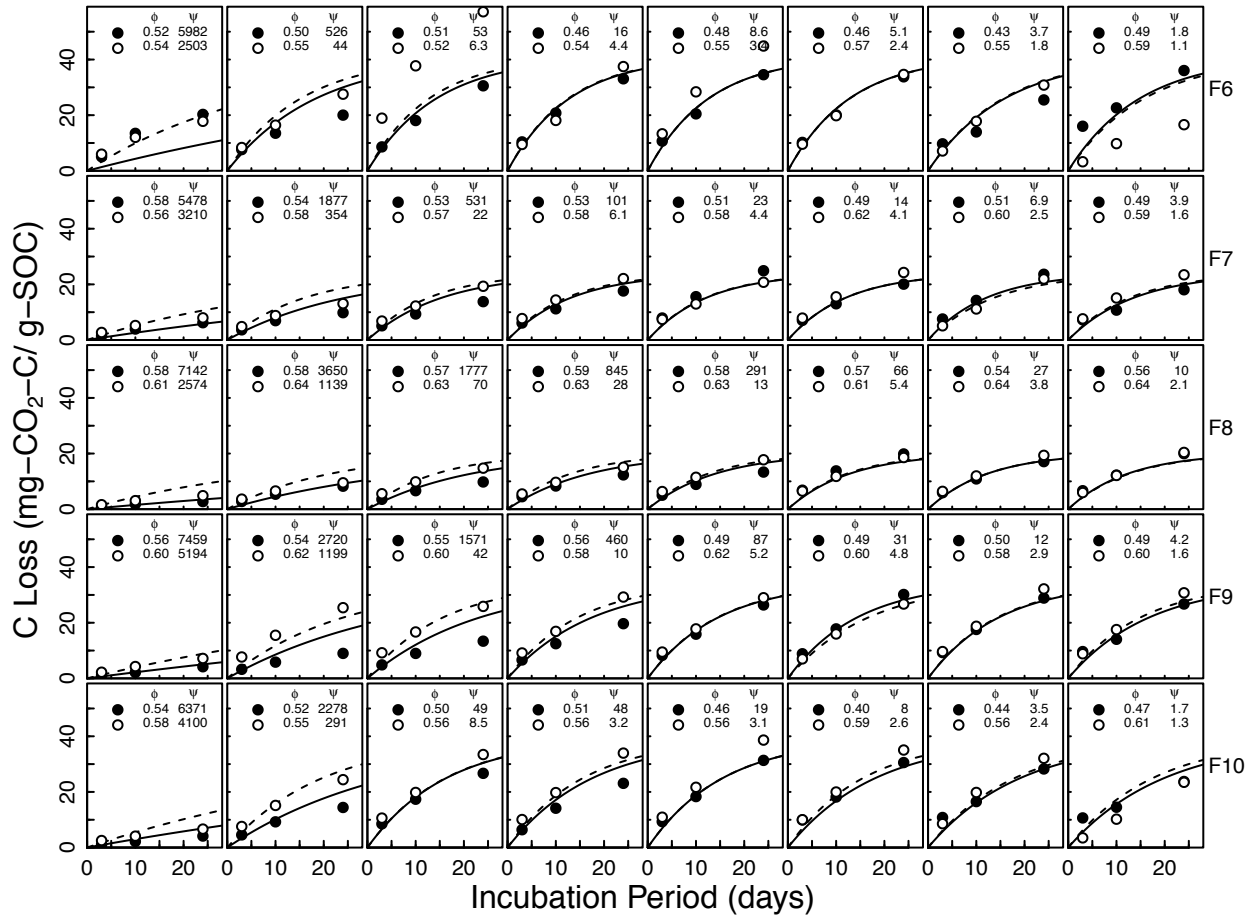


Figure A.3: (part 2/3) Decomposition experiments of Franzluebbers et al; fitted CO₂ evolution data. Fifteen different soils packed at two bulk density values incubated eight matric potential levels for 24 days. The porosity, water potential and RMSE of each sample are shown inside

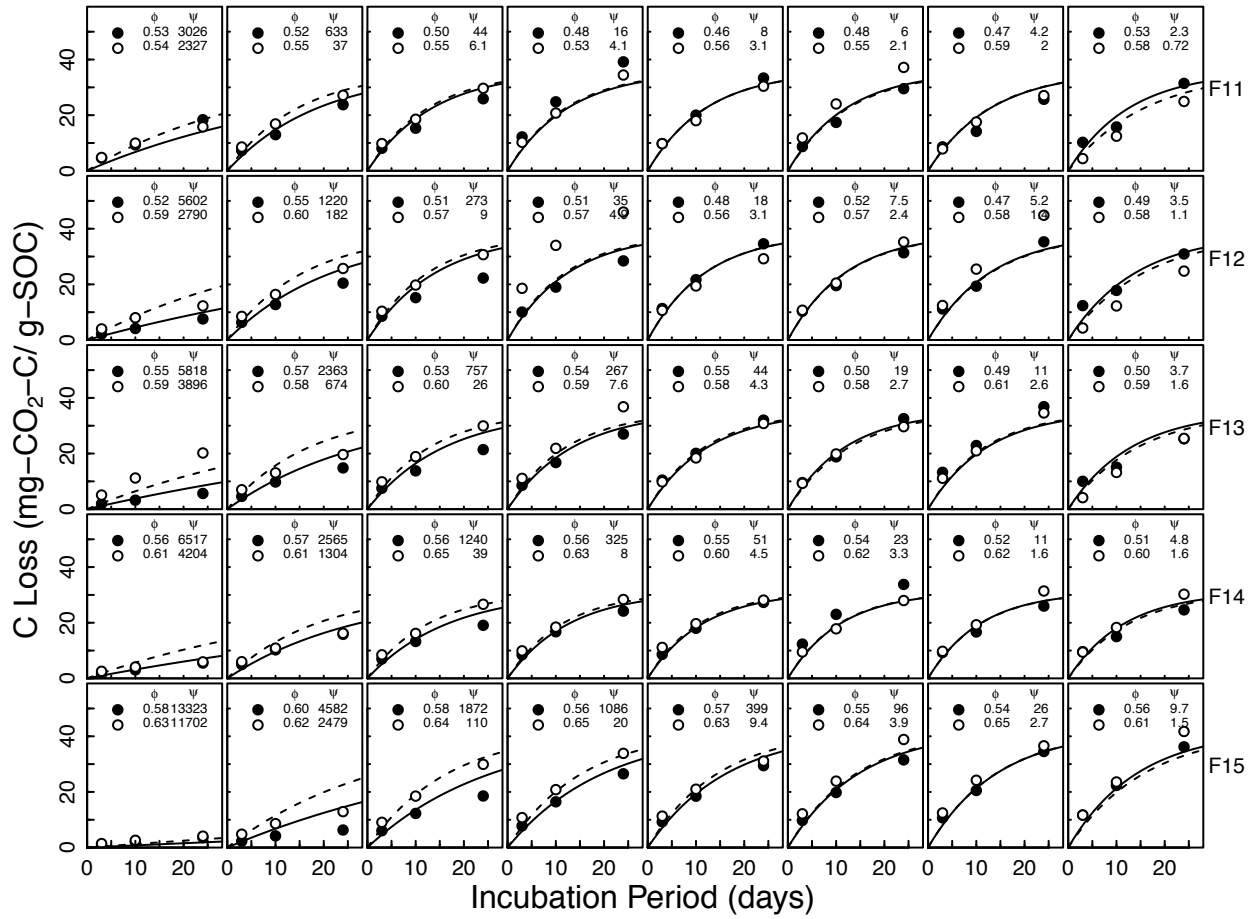


Figure A.3: (part 3/3) Decomposition experiments of Franzluebbers et al; fitted CO₂ evolution data. Fifteen different soils packed at two bulk density values incubated eight matric potential levels for 24 days. The porosity, water potential and RMSE of each sample are shown inside

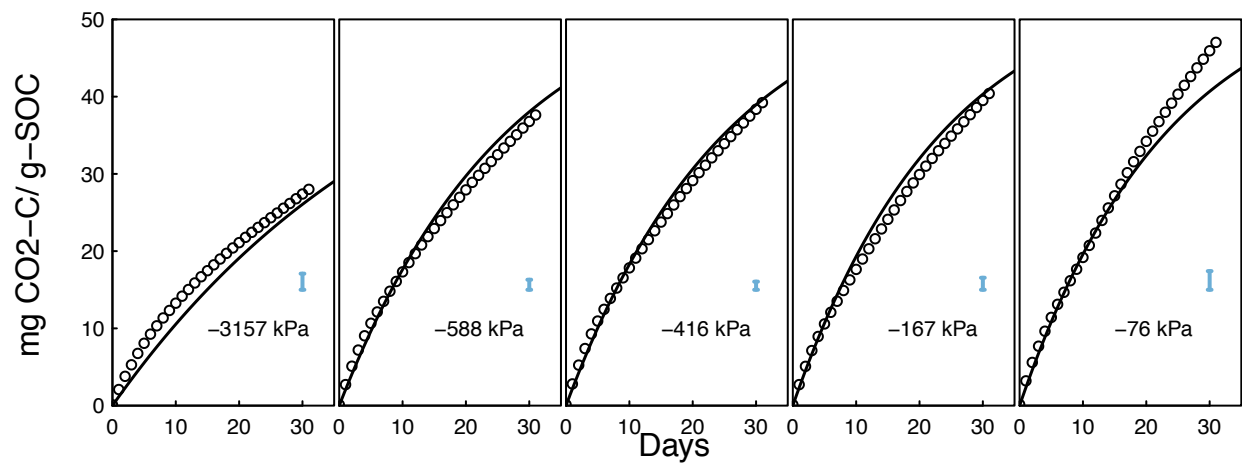


Figure A.4: Decomposition experiments of Don (data from Moyano); fitted CO₂ evolution data. Error bars denote RMSE. Soils from three hydrologic regimes and three depths incubated at five matric potentials for 400 days.

Table A1. Best Water Retention Curve and SOM dynamics model parameters

Soil Source and ID	Texture			K_0	C_0	θ_r	θ_s	van Genuchten		Durner					
	sand	silt	clay					SOC	α	n	α_1	n_1	α_2	n_2	
	sand	silt	clay	[g/g]	[yr $^{-1}$]	C_0	[–]	[–]	yr $^{-1}$	[–]	α_1	[–]	α_2	[–]	
Arnold D.B	0.650	0.260	0.090	0.025	0.005	0.132	NA	NA	NA	NA	0.004	1.330	0.413	5.000	0.282
Arnold D.M	0.650	0.270	0.060	0.033	0.009	0.125	NA	NA	NA	NA	0.002	2.556	0.397	3.194	0.231
Arnold D.T	0.670	0.280	0.050	0.057	0.010	0.135	NA	NA	NA	NA	0.003	1.660	0.376	4.557	0.344
Arnold I.B	0.610	0.320	0.070	0.023	0.003	0.189	NA	NA	NA	NA	0.003	1.974	0.395	3.684	0.265
Arnold I.M	0.640	0.310	0.050	0.032	0.004	0.156	NA	NA	NA	NA	0.005	1.490	0.338	4.629	0.227
Arnold I.T	0.710	0.230	0.060	0.104	0.011	0.145	NA	NA	NA	NA	0.007	1.301	0.386	4.176	0.300
Arnold W.B	0.730	0.250	0.050	0.103	0.001	0.237	NA	NA	NA	NA	0.003	1.753	0.391	3.545	0.173
Arnold W.M	0.640	0.320	0.040	0.126	0.001	0.500	NA	NA	NA	NA	0.002	3.896	0.404	2.735	0.214
Arnold W.T	NA	NA	NA	0.335	0.006	0.144	NA	NA	NA	NA	0.003	1.800	0.381	4.056	0.327
Don NA	0.807	0.103	0.090	0.011	0.146	0.064	0.050	0.407	0.351	1.763	NA	NA	NA	NA	NA
Franz. Comp. F_1	0.820	0.090	0.090	0.014	0.174	0.031	0.036	0.458	0.616	1.398	NA	NA	NA	NA	NA
Franz. Comp. F_2	0.760	0.120	0.120	0.015	0.150	0.034	0.048	0.480	0.315	1.523	NA	NA	NA	NA	NA
Franz. Comp. F_3	0.660	0.165	0.175	0.020	0.173	0.027	0.000	0.518	0.726	1.236	NA	NA	NA	NA	NA
Franz. Comp. F_4	0.710	0.100	0.190	0.011	0.211	0.038	0.020	0.439	0.226	1.336	NA	NA	NA	NA	NA
Franz. Comp. F_5	0.570	0.170	0.260	0.013	0.153	0.039	0.000	0.509	0.409	1.216	NA	NA	NA	NA	NA
Franz. Comp. F_6	0.775	0.125	0.100	0.014	0.152	0.041	0.035	0.480	0.565	1.415	NA	NA	NA	NA	NA
Franz. Comp. F_7	0.670	0.170	0.160	0.021	0.159	0.024	0.000	0.522	0.855	1.249	NA	NA	NA	NA	NA
Franz. Comp. F_8	0.510	0.275	0.215	0.029	0.156	0.020	0.000	0.570	0.770	1.223	NA	NA	NA	NA	NA
Franz. Comp. F_9	0.540	0.205	0.255	0.017	0.134	0.035	0.000	0.522	0.612	1.221	NA	NA	NA	NA	NA
Franz. Comp. F_10	0.610	0.145	0.245	0.012	0.124	0.039	0.017	0.479	0.486	1.320	NA	NA	NA	NA	NA
Franz. Comp. F_11	0.780	0.110	0.110	0.014	0.158	0.036	0.024	0.496	0.743	1.375	NA	NA	NA	NA	NA
Franz. Comp. F_12	0.725	0.125	0.150	0.015	0.161	0.038	0.018	0.506	0.698	1.307	NA	NA	NA	NA	NA
Franz. Comp. F_13	0.615	0.175	0.210	0.016	0.163	0.035	0.000	0.528	0.808	1.234	NA	NA	NA	NA	NA
Franz. Comp. F_14	0.535	0.220	0.245	0.019	0.179	0.031	0.000	0.547	1.015	1.233	NA	NA	NA	NA	NA
Franz. Comp. F_15	0.490	0.180	0.330	0.016	0.135	0.042	0.000	0.567	0.912	1.204	NA	NA	NA	NA	NA
Franz. Nat. F_1	0.820	0.090	0.090	0.014	0.174	0.031	0.052	0.458	0.527	1.694	NA	NA	NA	NA	NA
Franz. Nat. F_2	0.760	0.120	0.120	0.015	0.150	0.034	0.055	0.480	0.435	1.756	NA	NA	NA	NA	NA

Soil Source and ID	Texture			K_0	C_0	θ_r	θ_s	van Genuchten		Durner							
	sand	silt	clay					SOC	[g/g]	[yr $^{-1}$]	[-]	[-]	yr $^{-1}$	[-]	α_1	n_1	α_2
	sand	silt	clay														
Franz. Nat. F_3	0.660	0.165	0.175	0.020	0.173	0.027	0.059	0.518	1.365	1.374	NA	NA	NA	NA	NA	NA	NA
Franz. Nat. F_4	0.710	0.100	0.190	0.011	0.211	0.038	0.053	0.439	0.623	1.504	NA	NA	NA	NA	NA	NA	NA
Franz. Nat. F_5	0.570	0.170	0.260	0.013	0.153	0.039	0.046	0.509	1.318	1.310	NA	NA	NA	NA	NA	NA	NA
Franz. Nat. F_6	0.775	0.125	0.100	0.014	0.152	0.041	0.055	0.480	0.536	1.772	NA	NA	NA	NA	NA	NA	NA
Franz. Nat. F_7	0.670	0.170	0.160	0.021	0.159	0.024	0.059	0.522	0.834	1.479	NA	NA	NA	NA	NA	NA	NA
Franz. Nat. F_8	0.510	0.275	0.215	0.029	0.156	0.020	0.000	0.570	1.843	1.262	NA	NA	NA	NA	NA	NA	NA
Franz. Nat. F_9	0.540	0.205	0.255	0.017	0.134	0.035	0.000	0.522	2.141	1.237	NA	NA	NA	NA	NA	NA	NA
Franz. Nat. F_10	0.610	0.145	0.245	0.012	0.124	0.039	0.057	0.479	0.664	1.701	NA	NA	NA	NA	NA	NA	NA
Franz. Nat. F_11	0.780	0.110	0.110	0.014	0.158	0.036	0.056	0.496	0.662	1.709	NA	NA	NA	NA	NA	NA	NA
Franz. Nat. F_12	0.725	0.125	0.150	0.015	0.161	0.038	0.058	0.506	0.751	1.655	NA	NA	NA	NA	NA	NA	NA
Franz. Nat. F_13	0.615	0.175	0.210	0.016	0.163	0.035	0.059	0.528	0.829	1.499	NA	NA	NA	NA	NA	NA	NA
Franz. Nat. F_14	0.535	0.220	0.245	0.019	0.179	0.031	0.062	0.547	1.198	1.485	NA	NA	NA	NA	NA	NA	NA
Franz. Nat. F_15	0.490	0.180	0.330	0.016	0.135	0.042	0.063	0.567	1.886	1.358	NA	NA	NA	NA	NA	NA	NA